Sequence characterization of *T*, *Bip*, and *Phbw* demonstrates the role of MYB-bHLH-WD40 complexes and temperature in common bean seed color pattern formation

Travis Parker[1], Tayah Bolt[1], Troy Williams[1], R. Varma Penmetsa[1], Mwiinga Mulube[2], Antonia Palkovic[1], Celestina Nhagupana Jochua[3], Maria del Mar Rubio Wilhelmi[1], Sassoum Lo[1], Gail Bornhorst[4], Li Tian[1], Kelvin Kamfwa[2], Sam Hokin[5], Andrew Farmer[5], Christine Diepenbrock[1], and Paul Gepts[1]*

[1]Department of Plant Sciences, University of California, Davis, California, USA

[2]Department of Plant Sciences, School of Agricultural Sciences, University of Zambia, Lusaka, Zambia

[3]Instituto de Investigação Agrária de Moçambique (IIAM), Maputo, Mozambique

[4]Department of Biological and Agricultural Engineering, University of California, Davis, California, USA

[5]National Center for Genome Resources, Santa Fe, NM, USA
*Corresponding author. Email: plgepts@ucdavis.edu

ORCIDs:

Travis Parker 0000-0002-1233-7829

Tayah Bolt 0009-0008-4164-2436

Troy Williams: 0000-0003-2343-4293

R. Varma Penmetsa 0000-0001-8783-6334

Sassoum Lo 0000-0002-0385-5691

Gail Bornhorst 0000-0002-0852-826X

Li Tian 0000-0001-6461-6072

Kelvin Kamfwa 0000-0002-2375-9162

Maria del Mar Rubio-Wilhelmi 0009-0009-4884-2905

Paul Gepts 0000-0002-1056-4665

Word Count: 6,375 words

Number of Figures: 8

Number of Tables: 1

Supporting Information: number of Figures: 6; number of Tables: 4

Abstract

Seed colors and color patterns are critical for the survival of wild plants and the consumer appeal of crops. In common bean, a major global staple, these patterns are also critical for determining market classes, yet the genetic and environmental control of many pigmentation patterns remains unresolved. In this study, we genetically mapped variation for three important seed pattern loci, *T*, *Bip*, and p^{hbw}, which co-segregated completely with *PvTTG1*, *PvMYC1*, and *PvTT8*, respectively. Proteins encoded by these genes are predicted to work together in MYB-bHLH-WD40 (MBW) complexes, propagating flavonoid biosynthesis across the seed coat. Whole-genome sequencing of 37 diverse accessions identified putative mutations in each gene, including seven unique parallel mutations in *T* (*PvTTG1*) and a non-synonymous SNP in a conserved residue in bip^{ana} (*PvMYC1*). A 612 bp intron deletion in p^{hbw} *(PvTT8)* eliminated motifs conserved since the origins of the Papilionoidea and corresponded to a 20-fold reduction in transcript abundance. Mutations in MBW candidate genes for *Z* (*PvTT2*) and *Sellatus* (WDR) were also identified. In multi-location field trials with seven varieties with partial seed coat patterning, pigmented seed coat area was highly unstable and correlated with temperature, with up to 11-fold differences in pigmented area between the warmest and the coolest environments. In controlled growth chamber conditions, an increase of 4 °C was sufficient to cause pigmentation on an additional 21% of the seed coat area. Our results shed light on the fundamental activation of flavonoid biosynthesis in common bean and will be instrumental for maximizing consumer appeal in this nutritious staple crop.

Summary

- Seed colors and patterns are critical for the survival of wild plants, and are important in differentiating crop market classes, but the genetic control of these in the staple crop common bean (*Phaseolus vulgaris*) is largely unknown.

- The genetic, transcriptional, and environmental basis of common bean seed color patterning was explored through QTL mapping, whole-genome sequencing, RT-qPCR, and automated pigmentation quantification of seed grown in multi-location field trials and growth chamber environments.

- MYB-bHLH-WD40 complex-forming genes *PvTTG1*, *PvMYC1*, and *PvTT8* co-segregated completely with the color patterning genes *T*, *Bip*, and p^{hbw}. Mutations were identified in each gene, including seven unique parallel mutations in *T* (*PvTTG1*), a non-synonymous SNP in a conserved residue in bip^{ana} (*PvMYC1*), and an intron deletion in p^{hbw} *(PvTT8)* eliminating highly conserved motifs and corresponding to 20-fold lower *PvTT8* transcript abundance. Mutations in MBW candidate genes *Z* (*PvTT2*) and *Sellatus* (WDR) were also identified. In multi-location field trials, pigmented seed coat area was highly unstable and corresponded to temperature. In growth chamber conditions, an increase of 4 °C caused pigmentation on an additional 21% of the seed coat area.

- Our results highlight the critical interaction between MYB-bHLH-WD40 complex components and temperature in establishing seed pattern diversity.

Keywords

Domestication, MYB-bHLH-WD40, *Phaseolus vulgaris* (common bean), Pigmentation patterning, Seed color, Temperature effects, Transcription factor.

Introduction

Proper specification of pigmentation in tissues such as flowers and seed is essential for the survival of wild plants, and is critical for market acceptance of crops. In the wild, pigmentation is vital for pollinator attraction, camouflage of seed to reduce herbivory, and promotion of seed dispersal. During domestication, a radical change in selection criteria for plant color patterns occurred and domesticates have undergone a nearly universal color diversification of harvested organs (Darwin, 1868, Hufford et al. 2019). Despite this, within most individual cultures and markets, a narrow range of preferred colors and color patterns exists and types must fall within this range to be culturally accepted and commercially successful.

Among grain legume crops, the common bean (*Phaseolus vulgaris* L.) is the most important species for direct human consumption (Broughton et al. 2003, Parker and Gepts 2021). Consumers and farmers exhibit strong preferences for dry beans with specific colors and patterns (as well as seed shape and size), which together account for the wide diversity of seed types found in common bean and related grain legumes. Diverse common beans with novel seed patterns have undergone a resurgence in developed countries. Consumers are willing to pay a premium for specialty dry beans (Walters et al. 2011, Brouwer et al. 2016, Swegarden et al. 2016), offering a market opportunity for their production.

Unlike seed color patterns related to the complex *C* locus on chromosome Pv08, partial coloring related to genes such as *T*, *Bip*, and *P* is often maintained after cooking. Seed coat color is primarily due to pigmented phenolic compounds. Phenolics (including flavonoids, phenolic acids, and proanthocyanidins) are one of the largest classes of specialized metabolites in plants, are biosynthesized in the shikimate/phenylpropanoid pathway, and in common bean among other grain legumes, are primarily localized in the seed coats (Gálvez Ranilla et al. 2007, Singh et al. 2017). Alongside these aesthetic considerations, phenolics have antioxidant properties and other beneficial health effects (Kondratyuk & Pezzuto 2004, Gálvez Ranilla et al. 2007, Yang et al. 2018, Rodríguez-Madrera et al. 2020, Bai et al. 2023). Despite these and other important roles *in planta*, the genetic and environmental control of phenolic pigment biosynthesis is poorly understood in *Phaseolus* beans.

73 Several genes influence the production of phenolic pigments in common bean. These can
74 be classified into two major groups: a) factors controlling the spatial distribution of phenolic
75 pigments, including their presence or absence in given areas; and b) genes modifying the
76 composition (or visible color) of pigmentation uniformly throughout the seed coat. The first
77 category consists of several genes, including *Pigment* (*P*; Shull 1907, Koinange et al. 1996,
78 McClean et al. 2002, 2018). The *P* gene is dominant-acting and encodes a basic helix-loop-helix
79 (bHLH) protein that is necessary for color expression in seeds and flowers of common bean
80 (McClean et al. 2018). This gene is located on chromosome Pv07 and is orthologous to
81 *Arabidopsis thaliana TRANSPARENT TESTA 8* (*AtTT8*, McClean et al. 2018). While full loss-of-
82 function *p* alleles lead to complete loss of pigmentation in seeds and flowers, an allelic series of
83 four partial loss-of-function alleles also exists at *P*, leading to spatially restricted pigmentation
84 (Bassett 2007). This indicates that P is a spatial patterning gene, with full loss-of-function alleles
85 affecting phenolics production across all seed and floral tissues. Full loss-of-function *p* mutations
86 have arisen independently at least ten times (McClean et al. 2018).

87 Phenolic biosynthesis activation is also controlled by several other genes. The main factor
88 for this is *Totally* colored (*T*), which interacts with other genes such as *Bipunctata* (*Bip*), *Zonal*
89 (*Z*), and *Joker* (*J*) as the fundamental regulators of the presence or absence of pigment within any
90 given cell of the seed coat. The fully recessive *t* allele eliminates floral pigmentation, and in the
91 absence of secondary modifiers, may lead to a white patch of varying size opposite of the
92 chalazal side of the hilum (the "*expansa*" pattern; Ernest et al. 2005, their Fig 2). All other partly
93 colored patterns are achieved by *t* in combination with other mutations in *Bip, Z, J, Fib,* and/or
94 partial loss-of-function alleles at *P* (Bassett 2007). Allelic series have been described for *Bip* (*Bip*
95 $> bip^{ana} > bip$) and *Z* ($Z > z^{sel} > z$); with bip^{ana} leading to the anasazi pattern and z^{sel} leading to a
96 yellow eye-type *sellatus* pattern. The chromosomes associated with each gene have been mapped
97 through RAPD and STS markers (Brady et al. 1998, McClean et al. 2002, Reinprecht et al.
98 2013), but candidate genes for *T*, *Bip*, and *Z* are unknown, as are the molecular mechanisms of
99 these genes and of the partial loss-of-function alleles at *P*.

100 In Arabidopsis, biosynthesis of phenolics, particularly flavonoids, anthocyanins, and
101 proanthocyanidins, is under the control of MYB-bHLH-WDR (MBW) transcription factor
102 complexes (Baudry et al. 2004, Xu et al. 2015, Zhang and Schrader 2017). Among the most

important of these is the WDR-family gene *TTG1*, which combines with bHLH proteins such as *TT8* and *MYC1,* as well as numerous R2R3-MYB family transcription factors, including *TT2,* a critical flavonoid regulator (Baudry et al. 2004, Zhang and Schrader 2017). The complexes formed by these proteins further self-reinforce the expression of *TT8*, propagating the seed pigmentation signal from the chalaza through the rest of the seed coat (Baudry et al. 2006). These MBW complexes also activate expression of late biosynthetic genes (LBGs) related to phenolic production, including BANYULS (BAN, encoding anthocyanidin reductase; Baudry et al. 2004). Wu et al. (2019) and García-Fernández et al. (2021) characterized a cluster of *MYB113* homologs on Pv08 responsible for controlling the complex *C* pigmentation patterning locus of common bean. *MYB113* is an R2R3-MYB transcription factor and important MBW protein complex component; its homologs in cowpea control black seed color (Herniter et al. 2018). Similarly, the common bean seed color patterning gene *J* was recently linked to the R2R3-MYB transcription factor Phvul.010G130600 (Erfatpour et al. 2018, 2021; Erfatpour and Pauls 2020).

In this work, we seek to better understand the major regulatory factors influencing seed coat pigment biosynthesis in common bean. This entails the genetic mapping of several genes relevant to seed color in common bean, identification of interactions among these genes, whole-genome sequencing of 37 accessions with diverse seed color and patterns, gene expression analyses, and characterization of environmental effects on seed coat patterns in field research trials with growth chamber validation. Together, these results seek to answer fundamental questions about the control of seed patterning in common bean by interacting genetic and environmental factors.

Materials and Methods

Plant materials

The accessions 'Black Nightfall' (W6 51267) and 'Orca' (PI 632344, Hang et al. 2003) were used as parents in reciprocal crosses to develop a 217-member "BXO" recombinant inbred line (RIL) population (Parker et al. 2020). Black Nightfall has seed and floral patterns resembling the *half banner white* partial loss-of-function allele of *P* (p^{hbw}, Bassett 1996, 2003). Orca is a progeny of Anasazi with a similar pattern, making it likely to bear *P t* bip^{ana} (Bassett 2000). F_7 plants were field-grown in Davis, California, in 2018, and F_8 seeds were harvested and

132 phenotypically classified into one of six phenotypic categories based on seed and flower color. A
133 panel of 37 lines selected for seed color pattern diversity was used for whole-genome shotgun
134 sequencing. The partly-colored varieties 'Anasazi' (PI 577705), 'Orca', 'UC Southwest Gold' (PI
135 693470, Parker et al. 2021a), 'UC Southwest Red' (PI 693472, Parker et al. 2021b), 'UC Sunrise'
136 (PI 693474, Parker et al. 2021c), 'UC Four Corners Red' (PI 693469, T. Parker, unpublished),
137 'UCD Jacob's Cattle,' and 'UCD Holstein' (both S. Temple, unpublished) were used to evaluate
138 environmental impacts on seed color.

139

140 QTL mapping and identification of candidate genes

141 For QTL mapping, DNA was extracted from individual F_8 seeds of each line using a modified-
142 CTAB protocol (Allen et al. 2006). DNA quality was checked by NanoDrop spectrophotometer
143 and agarose gel electrophoresis and genotyped with the Illumina BARCBean6K_3 BeadChip
144 (Song et al. 2015), yielding 1164 segregating single-nucleotide polymorphisms (SNPs). Linkage
145 mapping was conducted using the ASMap R package (Taylor and Butler 2017, R Core Team
146 2022). QTL mapping was conducted on qualitative allelic states using maximum likelihood
147 through the EM algorithm of the R/qtl package in R (Broman et al. 2003). The 95th percentile of
148 1000 random permutations of the phenotypic data was used as a significance threshold (LOD =
149 3.03). The phenotype and genotype data at the most significant SNPs were compared to identify
150 SNPs flanking each seed coat patterning gene.

151 Descriptors and ontology information for all gene models between flanking SNPs of each QTL
152 were extracted from Phytozome 13 (Goodstein et al. 2012; Schmutz et al. 2014;
153 https://phytozome-next.jgi.doe.gov/info/Pvulgaris_v2_1). The amino acid sequences of
154 Arabidopsis seed coat pigmentation regulators were obtained from TAIR and searched by
155 BLASTp against the non-redundant proteomes of *P. vulgaris* and *A. thaliana*. Fast minimum
156 evolution trees were developed based on the Grishin protein matrix on the NCBI website
157 (BLAST: Basic Local Alignment Search Tool (nih.gov)) to compare patterns of sequence
158 similarity and homology.

159

160

Whole-genome sequencing and analysis

Whole-genome shotgun sequencing was conducted on the collection of 37 diverse accessions (Supporting Table S1) to better understand the sequence differences at candidate genes. DNA was extracted from seed embryonic axes of each variety using the Qiagen DNeasy Plant Minikit. Concentration and quality were checked by gel electrophoresis and Nanodrop, and the extracted DNA was sequenced by Illumina paired-end 150 bp sequencing at the UC Davis Genome Center. 270 Gb of sequence data were generated using a NovaSeq 6000 instrument, yielding an average of 12x sequencing depth per sample.

Sequence quality was checked with FASTQC (Andrews, 2010), and adapters and barcodes were trimmed using the Trimmomatic v0.39 (Bolger et al. 2014) ILLUMINACLIP function. Low-quality sequence was removed using the SLIDINGWINDOW:4:20 MINLEN:50 settings. Trimmed reads were aligned to the genomes of the Andean genotype G19833 v2.1 (Schmutz et al. 2014) and the Mesoamerican genotype UI111 v1.1 using the Burrow-Wheeler Aligner (BWA; Li and Durbin, 2009). Alignments were then imported and compared at regions of interest in the Integrative Genomics Viewer (IGV; Robinson et al. 2011). Predicted protein models were developed and visualized using the SWISS-MODEL Expasy web server [SWISS-MODEL (expasy.org)].

Marker development and validation in recombinant lines

To evaluate the genotype of RILs with recombination, missing data, or heterozygosity between the markers flanking identified QTL at candidate mutations, DNA was extracted using a rapid NaOH-based protocol (Stonehouse et al. 2022, https://tinyurl.com/v24wzz4y) from Black Nightfall, Orca, and 45 BXO RILs. For three RILs with heterogeneous seed, DNA was extracted separately for each phenotypic class. These 47 lines were genotyped at all three loci to determine patterns of cosegregation between candidate mutations and phenotype. PCR and restriction digests were performed using the primers, cycling conditions, and restriction digest protocols in Supporting Table S2. PCR products were run on a 2.5% agarose gel for 25 minutes and visualized on a UV transilluminator to score indel size or CAPS cleavage at loci of interest.

190 ## RT-qPCR and intron splicing

191 To quantify gene transcriptional patterns and evaluate patterns of intron retention or excision,
192 RNA was sampled from developing seeds of greenhouse-grown plants at two time points: 10
193 days after anthesis (seeds approximately 5 mm long, 30 mg) and 20 days after anthesis (seeds
194 approximately 10 mm long, 300 mg). Samples were flash-frozen in liquid nitrogen and
195 maintained at -80 °C. RNA was extracted with the Qiagen RNeasy Plant Mini kit, with
196 concentration and quality subsequently confirmed by NanoDrop and 1% bleach gel
197 electrophoresis. Reverse transcription was conducted with the Invitrogen SuperScript IV VILO
198 Master Mix and ezDNase kit. To evaluate the excision status of the second *TT8* intron, primers
199 were designed to span from the second to the third exon (Supporting Table 2). PCR was
200 performed on cDNA templates; the amplification product was run on a 2% agarose gel for 25
201 minutes and visualized on a UV transilluminator.

202 For RT-qPCR, transcript identifiers for each candidate gene were used to generate
203 primers in NCBI primer BLAST with specificity checking to avoid amplification of non-target
204 sequences. Intron-spanning primers were developed for all multi-exon genes, and controls
205 without reverse transcriptase were run. RT-qPCR was conducted using the Qiagen Quantinova
206 SYBR Green PCR Kit. The efficiency of qPCR primers was checked on pooled cDNA, and all
207 selected primer pairs were shown to amplify with an efficiency of 0.96-1.08. The difference in
208 C_T values between candidate and reference genes was used to generate ΔC_T data, which was then
209 logarithmically converted to $2^{-\Delta C_T}$ values. Differences in expression between phenotypic
210 groups were then compared by anova and LSD.test() in the agricolae R package (de Mendiburu
211 2019).

212

213 ## Environmental variables

214 To test for environmental factors affecting seed color, seven partly-colored varieties were field-
215 grown at four locations across a coastal vs. inland climatic gradient in California, USA. These
216 field sites were located in Pescadero (July average high/low: 21/11 °C; 37.223 °N, 122.359 °W;
217 grown 2019), San Juan Bautista (27/12 °C; 36.847 °N, 121.535 °W; grown 2018), Valley Center
218 (30/16 °C; 33.277°N, 117.026°W; grown 2018), and Davis (34/14 °C; 38.541 °N, 121.767 °W;
219 grown 2019). For all experiments, a randomized complete block design was used with three

220 replicated plots of 120 plants each. Seeds of each plot were bulk-harvested at dry maturity and
221 approximately 100 seeds per lot were scanned to quantify the percent of pigmented seed coat
222 area (PPSC). Scans were conducted using a Brother (Nagoya, Japan) DCP-7065DN scanner.
223 Custom macros were developed in ImageJ to quantify the PPSC and total seed coat area. The
224 quotient of these values was used to quantify the PPSC. The source code for the ImageJ macro is
225 available at https://github.com/TravisParker91/Seed-color. Differences in PPSC were compared
226 by two-way ANOVA with genotype and location as predictors and with an interaction term, and
227 the LSD.test() in the agricolae R package was used with a Bonferroni correction for comparison
228 of group means.

229 To test the isolated role of temperature on seed pigmentation, four plants of each of three
230 partly colored varieties with compact growth habit were grown in two identical growth chambers
231 of different temperatures, at 24/20 °C and 28/24 °C. Seeds were harvested from dry pods, and
232 seeds were scanned to quantify pigmentation and statistically analyzed according to the methods
233 used for field-grown seeds.

234

235 **Results**

236 Genetic component of seed pigment distribution

237 The BXO RIL population displayed transgressive segregation for seed and flower color, with
238 seeds ranging from entirely black to almost entirely white, and flowers ranging from solid purple
239 to white. In total, six unique seed/floral color classes were identified in the population. The
240 predicted allelic combinations of Black Nightfall (p^{hbw} *T Bip*) and Orca (*P t* bip^{ana}) were
241 assembled into a potential genetic segregation model (Fig. 1) based on known specific effects of
242 the three genes (Bassett 2007) and predictions of previously unstudied allele combinations (p^{hbw} *t*
243 bip^{ana}; p^{hbw} *T* bip^{ana}). These combinations fit expected frequencies for the proportion of RILs in
244 each category, supporting the model (χ^2 test: p=0.14).

245 Significant QTLs for p^{hbw}, *T,* and *Bip* were identified in the BXO population (Fig. 2). *T*
246 mapped to chromosome Pv09 between 8,427,110 and 9,220,699 bp (*P. vulgaris* G19833 genome
247 v2.1, Schmutz et al. 2014) (Table 1). This region included 63 predicted gene models, including
248 the candidate gene Phvul.009G044700, a WDR protein whose closest Arabidopsis relative is

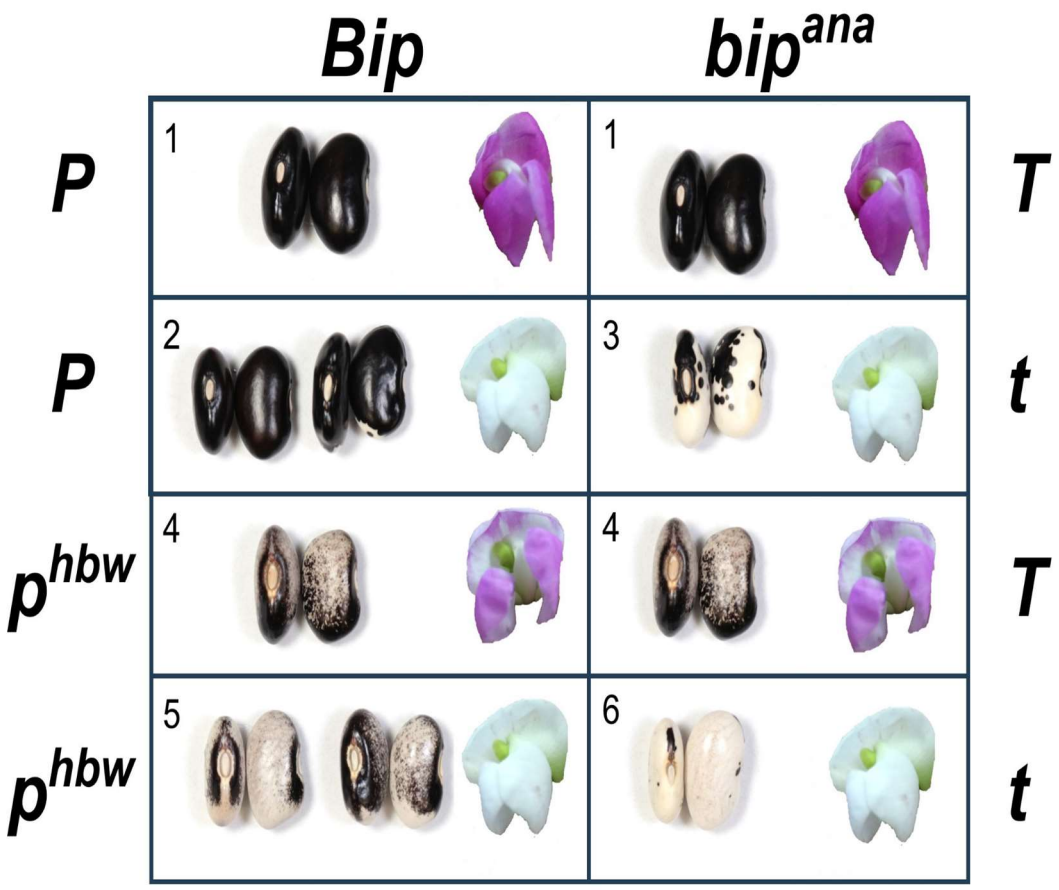

Fig. 1. Genetic model of seed and floral patterning in the Black Nightfall/Orca (BXO) recombinant inbred line (RIL) population of common bean (P. vulgaris) based on the segregation of three loci with two alleles each: 1) P, p^{hbw}; 2) Bip, bip^{ana}; and 3) T, t. Six main phenotypic categories were observed in the population. The parental phenotypes Black Nightfall and Orca correspond to segregation classes 4 and 3, respectively, and the population shows transgressive segregation beyond this range of seed color patterning.

TTG1 (Supporting Fig. S1), a major seed coat color regulator. Phvul.009G044700 was therefore designated *PvTTG1*. Nine RILs showed recombination between the flanking markers, and the SNP closest to *PvTTG1* (at 283 kb in physical distance) was also the SNP most closely associated with floral and seed color patterns influenced by *T* (LOD = 53.8).

Bip mapped to chromosome Pv10 between 35,632,623 and 36,893,960 bp, a region with 76 predicted genes. Among these was Phvul.010G098500, predicted to encode a bHLH protein.

Table 1. Proposed unique mutant alleles with sequences characterized for the first time in this study

Allele	Arabidopsis homolog	Proposed gene model[1]	Variant	Example germplasm	Associated QTL (significant interval, bp)
t^{Orca}	*TTG1*	Phvul.009G044700	39 bp deletion (del23_61)	Orca	Pv09: 8,427,110-9,220,699
t^{SYE}	*TTG1*	Phvul.009G044700	5 bp deletion (del422_426)	Steuben Yellow Eye	
$t^{Rockwell}$	*TTG1*	Phvul.009G044700	1 bp deletion (del749)	Rockwell	
t^{VA}	*TTG1*	Phvul.009G044700	1 bp deletion (del131)	Vermont Appaloosa	
$t^{Snowcap}$	*TTG1*	Phvul.009G044700	SNP (730G>A)	Snowcap	
t^{DG}	*TTG1*	Phvul.009G044700	Whole gene deletion	Dapple Grey	
t^{cf}	*TTG1*	Phvul.009G044700	UTR 14 Mb inversion	Jacob's Cattle Gold	
bip^{ana}	*MYC1*	Phvul.010G098500	SNP (650G>T)	Orca	Pv10: 36,099,863-36,771,237
p^{hbw}	*TT8*	Phvul.007G171333	612 bp deletion	Black Nightfall	Pv07: 28,312,574-29,971,196
$p^{Hystyle}$	*TT8*	Phvul.007G171333	Deletion of first two exons	Hystyle	
z	*TT2*	Phvul.003G132100	730G>A	Jacob's Cattle Gold	1.4 cM from 31,468,000; McClean et al. 2002
sel	WDR	Phvul.001G192200	Promoter deletion at (-149 to -624 before 5'UTR)	Steuben Yellow Eye	1.03 cM from 44,856,138; Bassett 1997

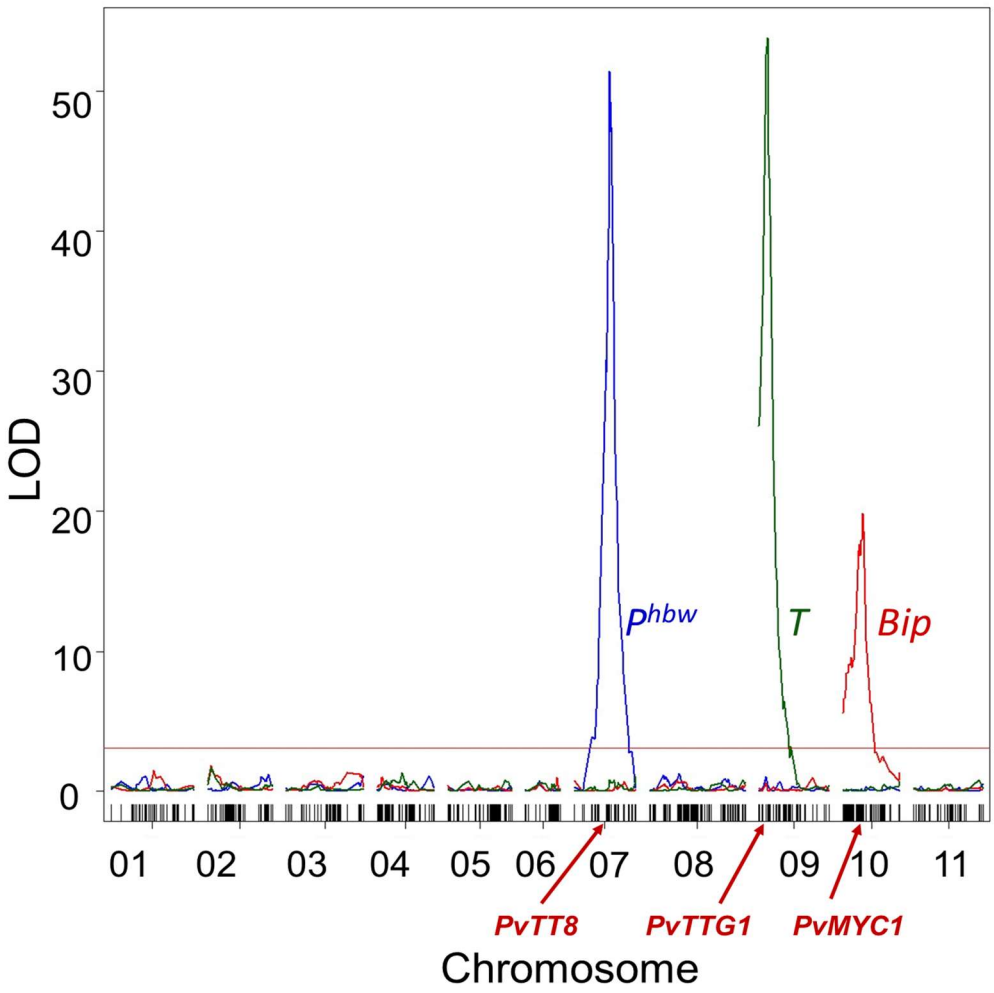

Fig. 2. QTL mapping of the three major pigmentation-related genes (*P*, *T*, and *Bip*) in the Black Nightfall x Orca recombinant inbred population based on the percentage of pigmented seed coat area (PPSC). In each case, the most significant SNP is also the marker closest in physical space to the putative gene. The horizontal red bar is the significance threshold (LOD=3.03) obtained by permutation tests. The red arrows point to the location of the candidate genes for the three genes.

256 Its protein product clusters as a sister clade to *MYC1* of Arabidopsis among all *A. thaliana* and *P.*
257 *vulgaris* proteins (Supporting Fig. S2). Phvul.010G098500 was therefore named *PvMYC1*.

258 In Arabidopsis, *MYC1* is known to form complexes with *TTG1* to specify seed coat color.
259 The SNP most strongly associated with *Bip* was found at 36,893,960 bp and was also the closest
260 SNP in physical distance to *PvMYC1* (LOD=19.9). A MYB transcription factor

261 Phvul.010G096400 was also found between the flanking markers. LOD scores for the QTL
262 containing *Bip* were lower than those for the QTL containing *T* or *P*. This is due to the hypostatic
263 nature of the gene relative to *T* (Fig. 1) as *Bip* could only be scored when *T* was homozygous
264 recessive (Figs. 1, 2). Five RILs carrying a homozygous recessive *t* locus showed recombination
265 between the flanking SNPs, and these were later screened for fine mapping at the candidate
266 mutation.

267 The p^{hbw} allele mapped to chromosome Pv07 between 28,312,574 (LOD=51.4) and
268 29,971,196, with 116 gene models and 16 gene models in the intervening space. This location is
269 consistent with the demonstrated allelism of p^{hbw} (formerly stp^{hbw}) and *P* (Bassett 2003), which
270 has previously been mapped to Phvul.007G171333 (*PvTT8,* McClean et al. 2018), a gene model

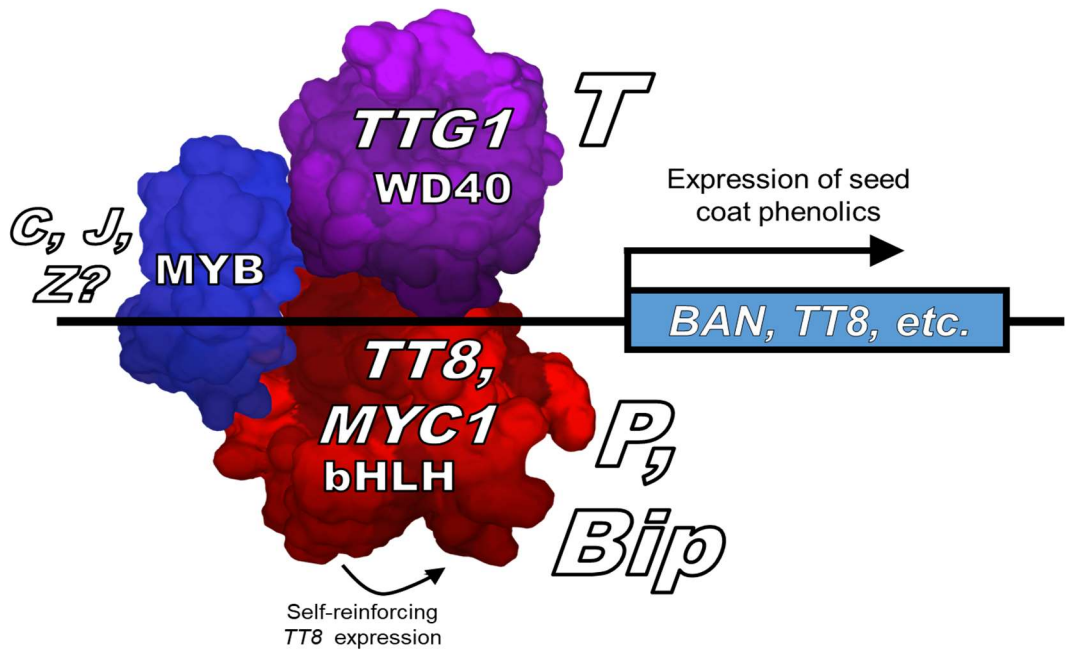

Fig. 3. Proposed molecular genetic model for MYB-bHLH-WD40 (MBW) complexes affecting the expression of flower and seed pigmentation genes in *Phaseolus vulgaris* (see also Fig. 1 as example). Mapped genes (*T*, *P*, *Bip,* and potentially *Z*, *J*, and *C*) are predicted to encode proteins that form MYB-bHLH-WD40 (MBW) complexes to activate flavonoid biosynthesis. In Arabidopsis, these require the inclusion of the WD40 protein *TTG1*, bHLH proteins such as *TT8* or *MYC1*, and any of several R2R3-MYB transcription factors. *PvTTG1*, *PvTT8*, and *PvMYC1*, are found between the QTL flanking markers for *T*, *P*, and *Bip*, respectively.

271 in this interval. Each of the identified candidate gene models are MBW complex members (Fig.
272 3).

273

274 Sequencing

275 Sequence analysis in the 37 varieties (Fig. 4) at *PvTTG1* identified seven unique mutations that
276 could explain loss of function in *T.* All partly-white seed types had one of these seven mutations,
277 whereas none of the mutations were found in any fully-colored lines. The mutations included 1)
278 a 39-bp deletion found in Orca and all five other Middle American partly-colored lines (t^{Orca}) , 2)
279 a 5-bp deletion found in Steuben Yellow Eye (t^{SYE}) and two other lines, 3) a single-base-pair
280 deletion found in Rockwell ($t^{Rockwell}$) and two other types, 4) a different single-base-pair deletion
281 found only in Vermont Appaloosa (t^{VA}), 5) a 1-bp, non-synonymous substitution in Snowcap
282 ($t^{Snowcap}$), 6) a 14-Mb inversion cutting into the 3' untranslated region (UTR) of UCD Holstein
283 and five other kidney-shaped lines with colored flowers (t^{cf}), and 6) a deletion of the entire gene
284 in Dapple Grey (t^{DG}).

285 The in-frame 39-bp t^{Orca} deletion found in Middle American lines leads to elimination of
286 residues 9-21 of the predicted protein product. These are found in one of the protein's WD40
287 domains, which spans amino acid positions 9-54. Seven of the 13 amino acids deleted are
288 conserved in alignments with *TTG1* in Arabidopsis. The three frameshift mutations (t^{VA}, t^{SYE},
289 $t^{Rockwell}$) all led to premature stop codons. Whereas the wild-type amino acid chain has 336 amino
290 acids, 254 are produced in $t^{Rockwell}$, 177 in t^{SYE}, and 94 in Vermont Appaloosa (Fig. 5). The
291 730G>A (D244N) substitution in $t^{Snowcap}$ affected a highly conserved residue, as Asp was the
292 only residue found at this position among the 100 most similar proteins in the NCBI reference
293 protein database, which included species of 21 plant families, indicating strong conservation and
294 deleterious effects of substitution. A SIFT (https://sift.bii.a-
295 star.edu.sg/www/SIFT_seq_submit2.html) analysis predicted that the D244N substitution would
296 not be tolerated, and that Asp was the only amino acid residue not predicted to negatively impact
297 gene function at the site. Types with the T^{cf} allele showed a sequence break in the 3' UTR, with
298 mate sequences on both sides of the junction pairing with a similar break 14 Mb downstream on
299 the chromosome, consistent with a major 14 Mb inversion. In Dapple Grey, *PvTTG1* was deleted

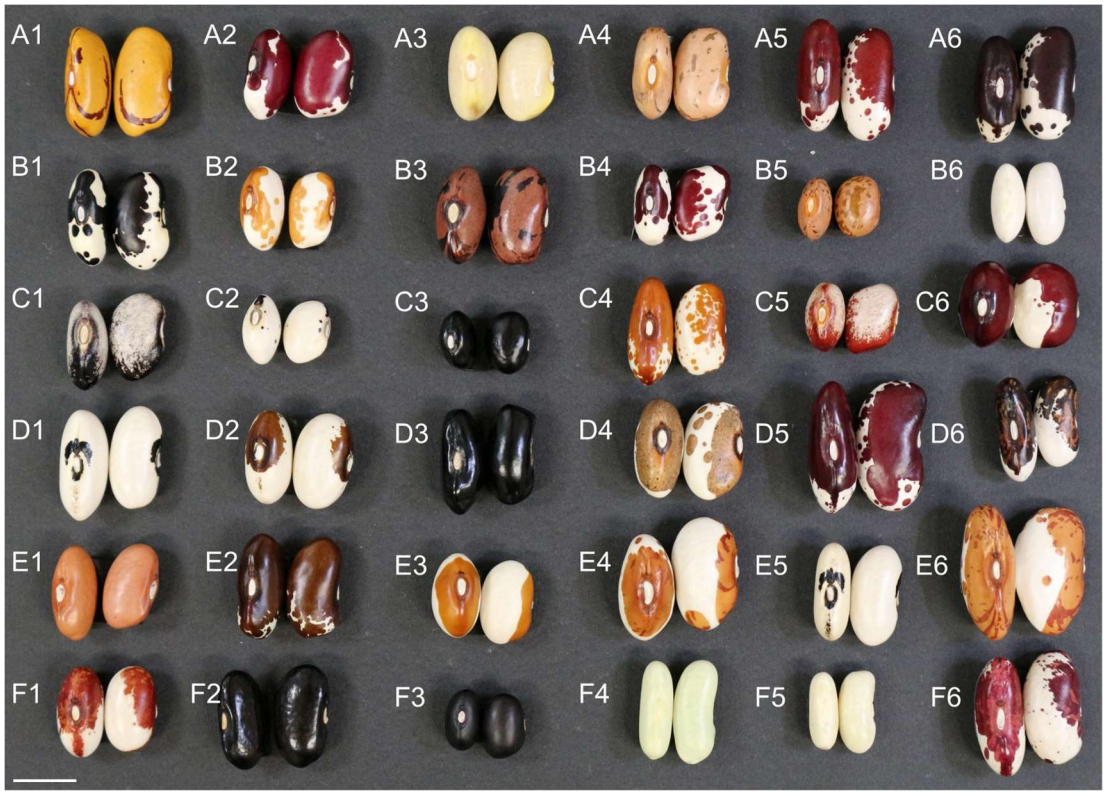

Fig. 4 Seed coat diversity among 36 accessions used for whole-genome sequencing. Varieties were sampled from both domesticated gene pools and across most major economic classes, with a particular emphasis on types with partially white seed coats. For each accession, two seeds are shown, displaying the hilum side and the other showing the lateral side, with the caruncula or chalaza oriented above the hilum. Partly colored seed coats are controlled by interactions between T and other genes such as Bip, Z, J, and certain alleles at P. A 37th accession (not pictured) was an isogenic line of entry F5 with the same seed type. A1: UC Tiger's Eye; A2: UC Four Corners Red; A3: UC Canario 707; A4: Bill Z; A5: UCD Jacob's Cattle; A6: UCD Holstein; B1: Orca; B2: UC Southwest Gold; B3: UC Rio Zape; B4: UC Southwest Red; B5: MCM5001; B6: Vanilla; C1: Black Nightfall; C2: BXO075; C3: OXB178; C4: Jacob's Gold; C5: Rio Colorado; C6: Red Calypso; D1: Improved Kidney Wax; D2: Davis; D3: Prolific Black Wax; D4: Dapple Grey; D5: Prefontaine; D6: Vermont Appaloosa; E1: UCD Pink 9634; E2: Pawnee Shell; E3: Steuben Yellow Eye; E4: Hidatsa Shield; E5: Burpee's Kidney Wax; E6: Snowcap; F1: Rockwell; F2: Best of All Stringless Wax; F3: UI-911; F4: Hystyle (N3); F5: Prevail (I23); F6: Great Lakes Special. A 37th accession (not pictured) was an isogenic line of Prevail with the same seed type. Scale bar represents 1 cm.

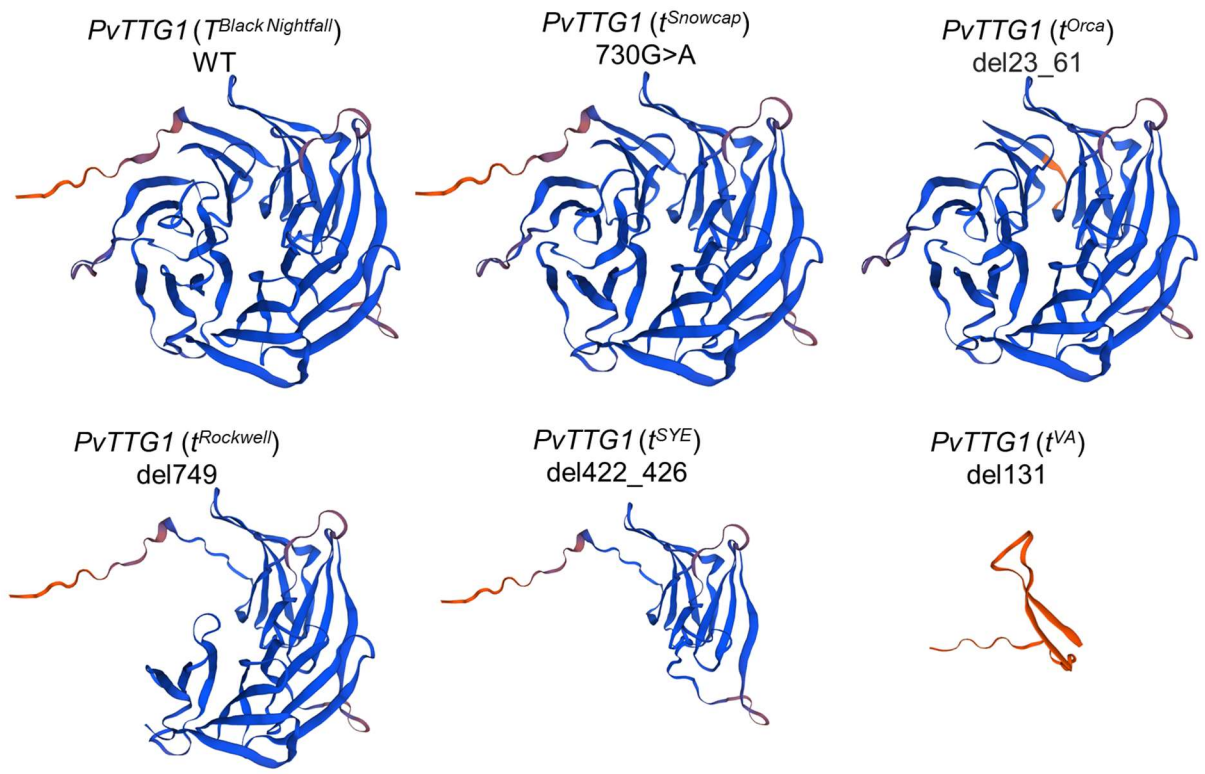

Fig. 5 Structural variation in *PvTTG1* (*T*) wild-type and mutant forms. A screen of 21 varieties with partly-colored seeds identified seven distinct parallel mutations in *PvTTG1* (Phvul.009G044700). These include a non-synonymous substitution tSnowcap, two separate deletions of a single base pair ($t^{Rockwell}$ and $t^{Vermont\ Appaloosa}$ = t^{VA}), a 5 bp deletion (*tSteuben Yellow Eye* = t^{SYE}), a 39 bp deletion (t^{Orca}), a 14 Mb inversion spanning into the UTR ($t^{cf,}$ not shown), and a deletion of the entire gene ($t^{Dapple\ Grey}$ = t^{DG}, not shown). Models were developed and visualized with the SWISS-MODEL Expasy web server (swissmodel.expasy.org).

in its entirety, with the deletion spanning from 15,507 bp upstream to 18 bp downstream of the gene.

Sequence evaluation of Phvul.010G098500 (*PvMYC1*) determined that Black Nightfall carried a race Mesoamerica haplotype at the locus, which differed from the race Durango haplotype carried by all five types with the Orca pattern. To identify polymorphisms related to bip^{ana}, these types were therefore compared against the sequence of the race Durango breeding line UCD Pink 9634, known to also have wild-type *Bip* (Parker et al. 2021a,b,c). The *PvMYC1* coding sequence, UTRs, and 500 bp upstream of the transcription start site (TSS) only differed

309 between wild-type UCD Pink 9634 and the mutant lines at two substituted base pairs. One of
310 these, 1640C>T, led to an A547V substitution in a poorly conserved site. Seven different amino
311 acids and a deletion occurred at this position across the 100 most similar protein models in the
312 NCBI reference protein database. In contrast, the second SNP, 650G>T, leads to a non-
313 synonymous C217F substitution at a highly conserved residue. Of the 100 most similar protein
314 models in the NCBI reference protein database, representing nine plant families, 98 had cysteine
315 residues at this site. The two exceptions were alternately spliced isoforms of a single soybean
316 gene (Glyma.03G009500) which maintains the Cys in its primary transcript. No proteins in the
317 database showed a non-synonymous substitution or deletion of the nucleotides encoding the Cys
318 at position 217, indicating that the 650G>T substitution is highly likely to impact gene function.
319 In contrast to *PvMYC1*, Phvul.010G096400 contained no non-synonymous SNPs or variation
320 within 500 bp upstream of the TSS that distinguished Black Nightfall and Orca.

321 The three varieties displaying p^{hbw} phenotypes (Black Nightfall, Rio Colorado, and the
322 triple-mutant RIL BXO075) shared a 612 bp deletion from positions 19-630 bp in the second
323 intron of Phvul.007G171333. This deletion was not identified in any other accessions in the
324 panel. To identify and assess conserved regulatory motifs in the area, sequence data from the
325 closest homologs of the gene across all legume species with above-ground seeds in the
326 Phytozome database were extracted. BLAST sequence alignments identified motifs in the intron
327 region that were conserved across all species analyzed (Supporting Fig. S3), except for the non-
328 papilionoid legume *Cercis canadensis* (Koenen et al. 2021). The conservation of these intron
329 motifs across all papilionoids, including those of the cool-season inverted repeat-lacking (IRLC)
330 clade and the basal species *Lupinus albus*, contrasted with what was seen in other introns, which
331 were weakly conserved. Intriguingly, homologous introns in the partly-colored reference lima
332 bean accession G27455 and partly-colored reference cowpea accession IT97K-499-35 also
333 display deletions in overlapping areas, where other members of each species show the full intron
334 with conserved motifs (Supporting Fig. S3). The three sequenced varieties of snap (green) bean
335 also shared a unique and previously undescribed full loss-of-function mutation at *P*, consisting of
336 a deletion eliminating the first two exons of the gene and causing the desired, white-seeded
337 phenotype in this class.

338 Markers were successfully screened for the candidate mutations in *PvTT8, PvTTG1*, and
339 *PvMYC1* across Black Nightfall, Orca, and a panel of 49 genetically distinct BXO lines. For all
340 three genes, complete co-segregation was found between the genotype at the candidate mutations
341 and color pattern phenotype. This co-segregation was found in all 16 recombinant RILs for *P*, in
342 9 for *T*, and in 5 for *Bip*. For *Bip*, marker screening and recombinants also removed from
343 consideration the MYB Phvul.010G096400 gene model and all genes further upstream due to
344 recombination in BXO140, and Phvul.010G100300 and genes further downstream based on the
345 WGS data of BXO075. This limited the Bip interval to 39 genes, including *PvMYC1*.

346

347 Gene expression and *PvTT8* intron splicing

348 In seeds sampled 20 days after anthesis, the expression of Phvul.007G171333 (*PvTT8, P,* Fig. 6)
349 differed significantly between phenotypic groups (P=0.002, ANOVA). *P* expression was
350 significantly higher in types with wild-type *P* and *T* (phenotypic class 1, full-colored black
351 seeds) than in any phenotypic class with the p^{hbw} partial loss-of-function allele (phenotypic
352 classes 4-6; Fisher's Least Significant Difference test, $\alpha = 0.05$). With dominant *T*, the p^{hbw} intron
353 deletion is associated with a 19.5-fold reduction in *P* expression relative to types without the
354 deletion (Fig. 6). *P* expression in *P T* genotypes was also 8-fold higher and non-overlapping with
355 that of *P t* genotypes. Despite this, *P t* types were intermediate in *P* expression and did not
356 significantly differ from any phenotypic categories in *P* expression. No significant differences in
357 the expression of *T* or *Bip* were identified, nor were any differences in gene expression identified
358 in seed samples collected 10 days after anthesis. Amplification of the *PvTT8* region spanning
359 from exon 2 to exon 3 using cDNA templates found uniform excision of intron 3 across *P* and
360 p^{hbw} types, indicating that the 612 bp deletion in the second intron observed in Black Nightfall
361 and two other lines does not affect intron splicing.

362

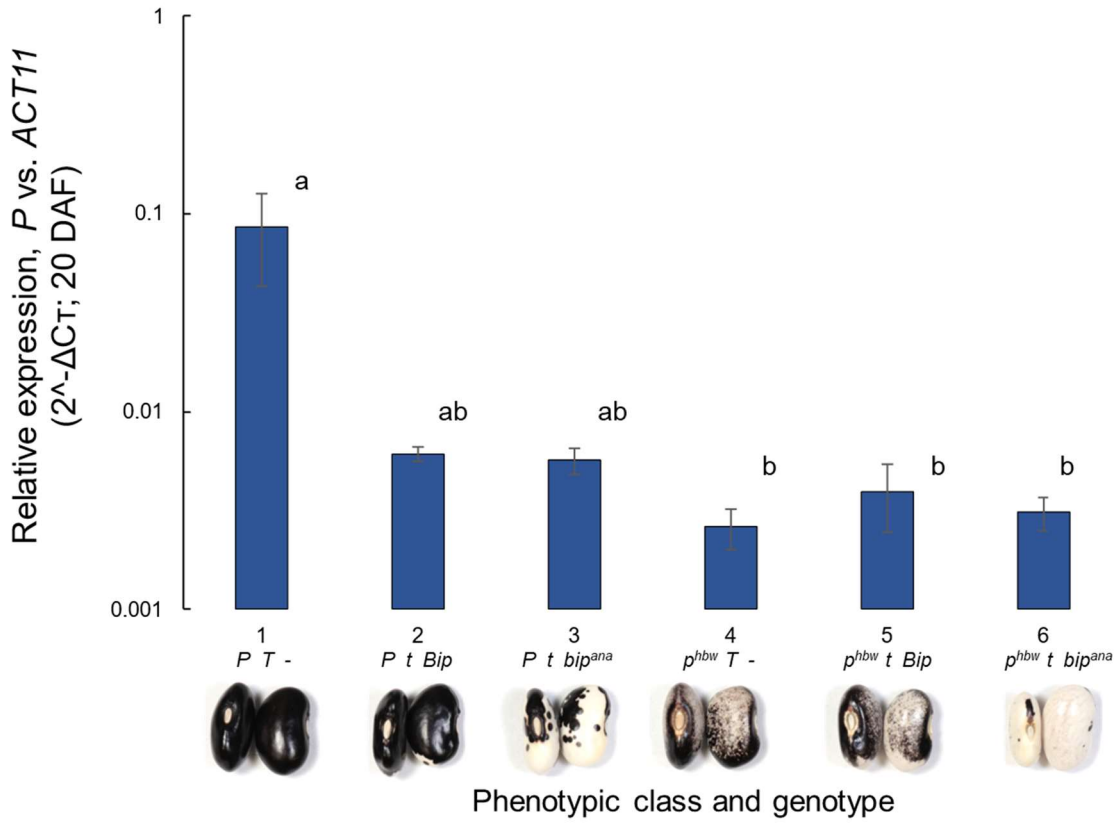

Fig. 6 Expression of P differed significantly across BXO phenotypic classes at 20 days after anthesis (P=0.002, ANOVA). RILs with *T* p^{hbw} carry a 612 bp intron deletion in *PvTT8* (phenotype class 4) and have 19.5-fold lower P expression than those with *P T* (phenotype class 1, see Fig. 1). *P* expression in genotypes with *P T* (phenotype class 1) was 8-fold higher and non-overlapping with that of types with *P t* (phenotype classes 2 and 3), indicating that *T* may also impact *P* expression. Bars represent standard error based on three replicates. Significance groups based on Fisher's Least Significant Difference test (α = 0.05).

Exploration of candidate genes for *Z* loci

The whole-genome sequencing of 37 diverse accessions allowed for the evaluation of other candidate genes that may control the broad seed color diversity of common bean. BLASTp indicated that common bean gene most similar to the critical Arabidopsis MYB gene *AtTT2* was Phvul.003G132100, *AtTT2* was also the most similar Arabidopsis protein to Phvul.003G132100 (Supporting Fig. S4). Phvul.003G132100 was therefore named *PvTT2*. Phvul.003G132100 is

370 found 1.4 Mb from OAM10[560], a marker previously mapped 1.4 cM from *Z* (McClean et al.
371 2002; 31.5 Mb on Pv03). Phvul.003G132100 expression is 22-fold higher in developing seeds
372 compared to any other tissue (O'Rourke et al. 2014; Supporting Figure S5), consistent with a
373 role in the regulation of seed-specific pigmentation. As a candidate gene for *Z*, the whole-
374 genome sequencing data were inspected at this gene model to identify polymorphisms that might
375 be related to seed color patterning.

376 In 22 Andean accessions, a 315G>T substitution was identified in the Phvul.003G132100
377 CDS, leading to the substitution of a Lys with an Asn (K105N). This residue is part of the MYB
378 domain of the protein, a region that extends from positions 62-116. The reference genome
379 G19833 (fully-colored Andean genotype) included a Lys at this position, as did the fully-colored
380 Andean variety UCD Canario 707 and all sequenced Middle American genotypes. In contrast, all
381 but one partly-colored Andean types had the Asn at this position. The one partly-colored Andean
382 type without this allele, Vermont Appaloosa, shows the *expansa* pattern consistent with *t Z*
383 (Bassett 2007). To determine the functional importance of the substitution based on sequence
384 conservation, BLASTp was used to align the G19833 amino acid sequence against the NCBI
385 RefSeq protein database. The 100 most similar proteins, spanning 16 plant families, all
386 maintained a Lys at the position. This extremely strong conservation suggests that substitutions
387 at the site have major deleterious effects on protein functionality. These results were further
388 tested using SIFT (https://sift.bii.a-star.edu.sg/www/SIFT_seq_submit2.html). The test results
389 indicated that only Lys would be tolerated at the position (threshold = 0.05, SeqRep = 0.87).

390 While the variation between *Z* and *z* was mapped to Pv03, the variation between *z* and z^{sel}
391 has historically been mapped to 1.03 ± 0.33 cM of the *fin* determinacy locus (Bassett 1997). The
392 *fin* locus has subsequently been characterized as *PvTFL1y* (Phvul.001G189200) on Pv01
393 (Repinski et al. 2012, Kwak et al. 2012), calling into question the localization of genetic factor(s)
394 comprising the reported allelic series for *Z*. Phvul.001G192200, a WD40 repeat protein and close
395 relative of *T*, was identified 245 kb from *fin* on Pv01. Expression patterns of the gene closely
396 resembled those of the *Z* candidate Phvul.003G132100 and *P* (Phvul.007G171333), with
397 expression in developing seeds 41-fold higher than in any non-seed tissue (Supporting Fig. S5,
398 O'Rourke et al. 2014). The four varieties with the *sellatus* pattern (Steuben Yellow Eye, Red
399 Calypso, Snowcap, and Hidatsa Shield; Fig. 4 C6, E3, E4, E6) all showed a single haplotype at

Phvul.001G192200, including a deletion of 477 bp from -149 to -641 bp upstream of the TSS. This variant was not found in any other sequenced lines.

Environmental component of seed pigment distribution

The proportion of pigmented seed coat (PPSC) varied significantly based on both genotype and environment. In the field, the difference in PPSC between varieties was highly significant ($P <$ 2.2e-16; Fig. 7), as were the differences based on environment ($P <$ 2.2e-16, two-way ANOVA). The interaction between genotype and environment was also highly significant (P =2.9e-14, two-way ANOVA). The greatest range in PPSC between environments was seen in the cultivar Orca, which produced pigment on 7±0.3% of the seed coat in the cool climate of Pescadero, CA, compared to 79±5% in the warmer climate of Davis, CA (Fig. 7b). The three varieties with compact growth habit (Orca, UC Southwest Gold, and UC Southwest Red) each had a significantly lower PPSC than any of the four vine types (Zuni Gold, Anasazi, UC Sunrise, UC Four Corners Red; Fisher's LSD). Location rankings by temperature were the same as by PPSC (Fig. 7b, Supporting Table S3, Supporting Fig. S6). This raised the hypothesis that temperature may have a direct effect on the regulation of pigmentation.

In identical growth chamber conditions varying only in temperature, the effect of temperature on the PPSC was highly significant (P = 9.33e-08, two-way ANOVA), as was the effect of genotype (P = 2.65e-09, two-way ANOVA) and genotype by environment interaction (P = 0.002, two-way ANOVA). A temperature difference of just 4 °C between the chambers was sufficient to cause pigmentation over an additional 20% of seed area on average across varieties (Fig. 7d). Seeds (P = 0.002, two-way ANOVA). A temperature difference of just 4 °C between the chambers was sufficient to cause pigmentation over an additional 20% of seed area on average across varieties (Fig. 7d). Seeds grown in the cooler chamber produced pigmentation on 71% of the seed coat, whereas 91% of the seed area was pigmented in the warmer chamber (Supporting Table S4).

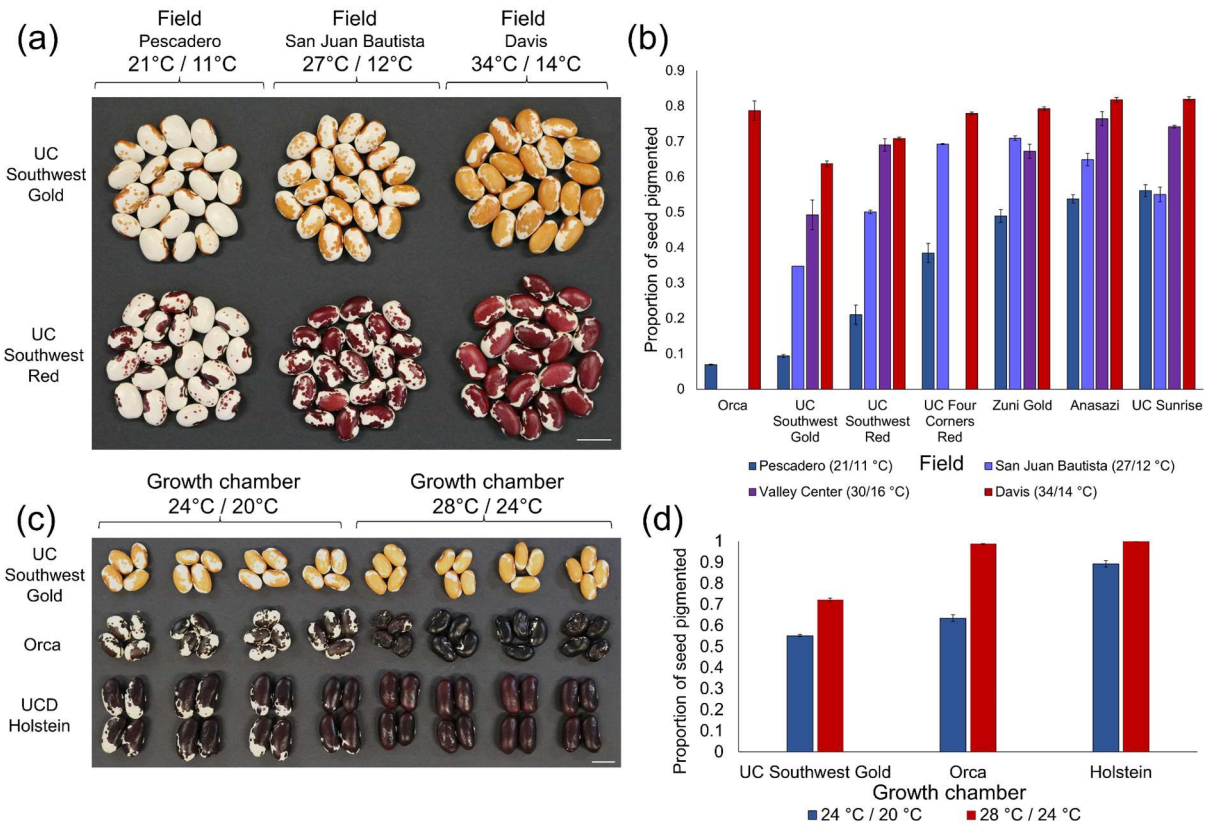

Fig. 7 Proportion of pigmented seed coat changes with temperature in field and growth chamber conditions. a) and b) Seeds grown in multi-location field trials (all California, USA) showed significant differences in seed coat pigmentation across environments, with up to 11-fold differences in the proportion of pigmented seed coat between the coolest and warmest environments (July average high/low temperatures shown, °C). c) and d) Growth chamber studies confirm that variation in temperature alone is sufficient to change proportion of seed coat pigmented. A difference of 4 °C was sufficient to cause pigmentation over 20% of the seed coat. Field experiments: 3 bulk-harvested plots per genotype per location; growth chamber: 4 individually harvested plants per genotype per temperature. Error bars represent standard error of the mean. Scale bars are 1 cm.

425

426 # Discussion

427 ## Genetic effects

428 Our mapping and sequencing results strongly indicate that a series of mutations have occurred
429 within each component of the MBW complexes and that these are responsible for a broad array
430 of color patterns in common bean. In *PvTTG1*, a series of at least seven parallel mutations
431 underpin the loss of function at the *T* locus and are found in all types with partially white seed
432 coats in the species. The identification of these seven separate mutations among the 22 partly-
433 colored accessions in our panel is compelling evidence for strong evolutionary parallelism for
434 the control of seed pattern diversification. These findings coincide with parallel molecular
435 evolution described for other loci in the species, such as *PvTFL1y* (Kwak et al. 2012), *PvTT8*
436 (McClean et al. 2018), and *PvPHYA* (Weller et al. 2019). This evolutionary parallelism also
437 extends to cowpea, in which mutations in the *TTG1* homolog (Vigun09g139900) and secondary
438 genes are required for partial white seed color (Herniter et al. 2019). This is an example of the
439 molecular basis of the law of homologous variation between species (Vavilov 1922).

440 Our results also indicate that *PvMYC1* likely underlies *Bip*. The bip^{ana} C217F substitution
441 identified in *PvMYC1* was found in all sequenced partly-colored Middle American varieties,
442 whereas no mutations were identified in the gene in Andean lines. These instead demonstrated
443 mutations at *PvTT2*. The C217F *PvMYC1* substitution occurs in a domain that interacts with
444 WD40 proteins in the related protein *AtTT8* (Zhai et al. 2019). Since the effects of bip^{ana} are
445 visible only with recessive *t* (a WD40 protein), the bip^{ana} mutation could achieve its effect due to
446 poor complex formation with the t^{Orca} protein variant, with poor binding affinity exacerbated by
447 low temperature. Alternatively, in the absence of a functional *T*, bip^{ana} may be poorer at binding
448 with alternate WD40 proteins to rescue pigmentation. These alternatives could be evaluated
449 through hybridization with varieties like Dapple Grey, which lacks *PvTTG1* in its entirety. The
450 existence of varieties with a full loss-of-function allele *bip* (Bassett 2007) and their difference in
451 phenotype compared to lines with the bip^{ana} allele indicates that the bip^{ana} allele likely retains
452 some functionality.

453 Our characterization of p^{hbw} sheds light on the partial loss-of-function allelic series at the
454 *P* locus. The conservation of specific motifs in intron 2, as well as the repeated loss of these
455 motifs in partly-colored accessions across three species, and expression differences between *P*

456 alleles, together strongly indicate that this intron contains functionally significant regulatory
457 sequences. The identification of overlapping intron deletions in the homologous genes of partly-
458 colored lima bean (Pl07G000031200) and cowpea (Vigun07g110700) indicates that these may be
459 important for color pattern regulation in these related species as well.

460 Our sequencing results also shed light on the nature of *Z*. Here, we propose a two-gene
461 model for the *Z*-associated phenotype instead of an allelic series. The identification of two
462 further candidate gene models closely related to *TTG1* (Phvul.001G192200) and *TT2*
463 (Phvul.003G132100), each located in close proximity to mapped "*Z*" alleles, each with nearly
464 seed-specific expression, and each with polymorphisms relating to phenotypic patterns, together
465 makes these compelling candidates for the control of *Z*-related seed color expression. According
466 to a single-gene model, types such as Steuben Yellow Eye (*sellatus* pattern) and Improved
467 Kidney Wax (*virgarcus* pattern) would be expected to differ at *Z* (Bassett 2007, Ernest et al.
468 2005). Our sequencing results, however, found a single identical mutation in both lines. These
469 *sellatus* and *virgarcus* types were, however, differentiated by the 477 bp deletion upstream of
470 Phvul.001G192200, which is tightly linked to the *PvTFL1y* locus tied to this variation previously
471 (Bassett 1997). We propose to call this Pv01 locus, hypostatic to *Z*, *Sellatus*. A two-gene model
472 for *Z*, rather than an allelic series at a single locus, would parallel the recent breakdown of allelic
473 series at both *bc-1* and *bc-2*, also in common bean (Soler-Garzón et al. 2021a,b).

474

475 Expression and intron splicing

476 Our expression analyses indicate that the loss of the 612 bp intron fragment in p^{hbw} types
477 corresponds with a 19.5-fold reduction in *P* transcription. The critical role of intron motifs in
478 promoting transcription is becoming increasingly clear; for many genes, intron motifs are more
479 important for transcriptional regulation than sequences upstream of the TSS (Rose 2019). The
480 non-overlapping and 8-fold lower expression of *P* in genotypes with $P\ t^{orca}$ indicates that *T* may
481 also regulate *P* expression, as proposed before the genomics era by Bassett (2003). This fits with
482 the pattern of Arabidopsis, in which *TT8* expression—but not expression of *TTG1* or *MYC1*—is
483 known to be self-reinforced through a positive feedback mechanism by MBW complexes
484 (Baudry et al. 2006). The lack of differential expression of *T* and *Bip* also fits with our
485 sequencing results, in which the *t* and bip^{ana} mutations of the BXO population affect protein

486 sequence rather than protein abundance. The finding of significant expression differences for *P*
487 only at the later sampling time point, together with the seed coloration patterns of single, double,
488 and triple mutants, is consistent with a model in which the MBW complexes of *Phaseolus*
489 *vulgaris* propagate pigmentation from the chalaza through the rest of the seed coat. This parallels
490 what has been identified in the development of Arabidopsis seeds (Baudry et al. 2006) and
491 phenotypic descriptions of patterns observed in cowpea (Herniter et al. 2019).

492

493 ## Environmental effects

494 Our field and growth chamber studies show compelling evidence that temperature affects the
495 MBW complexes that regulate pigment biosynthesis in partly-colored varieties. In field
496 conditions, the PPSC in Orca varied by 70% between the warmest and coolest conditions,
497 suggesting that activation of flavonoid biosynthesis might be disrupted at low temperatures.
498 These results were confirmed in carefully controlled growth chamber conditions, which isolated
499 temperature as the sole variable. In these conditions, a difference of 4 °C was sufficient to cause
500 a 20% difference in the PPSC, in line with the findings of the field-based studies. This instability
501 may be a hindrance to the large-scale commercialization of partly white-seeded varieties, which
502 are characteristic of some heirloom or specialty bean types but which have been poorly
503 incorporated into large-scale commercial operations where high uniformity is expected. The
504 higher stability of vine-type varieties across temperatures may be explained by differences in pod
505 placement, with pods developing closer to the soil surface and at higher temperatures than those
506 of upright bush types.

507 Temperature has a strong effect on protein-protein interactions (e.g., Xie et al. 2012). The
508 strong environmental effects of *t*-related seed coat mottling are consistent with a model in which
509 low temperatures disrupt MBW complex activity, causing a failure of signal propagation
510 throughout the seed coat (Fig. 8). This is also consistent with the localization of the putative
511 mutations in *PvMYC1*'s WD40-interacting domain, as well as deletion of part of a WD40 repeat
512 domain in Orca. Alternatively, temperature may affect transcription directly through differential
513 binding of transcription factors to regulatory sequence or other means. Environmental testing
514 was conducted with types carrying t^{orca} bip^{ana} or t^{cf} *z*, but similar evaluations could be conducted
515 with other mutations at *t, bip*, and *z* to determine whether other alleles (and combinations

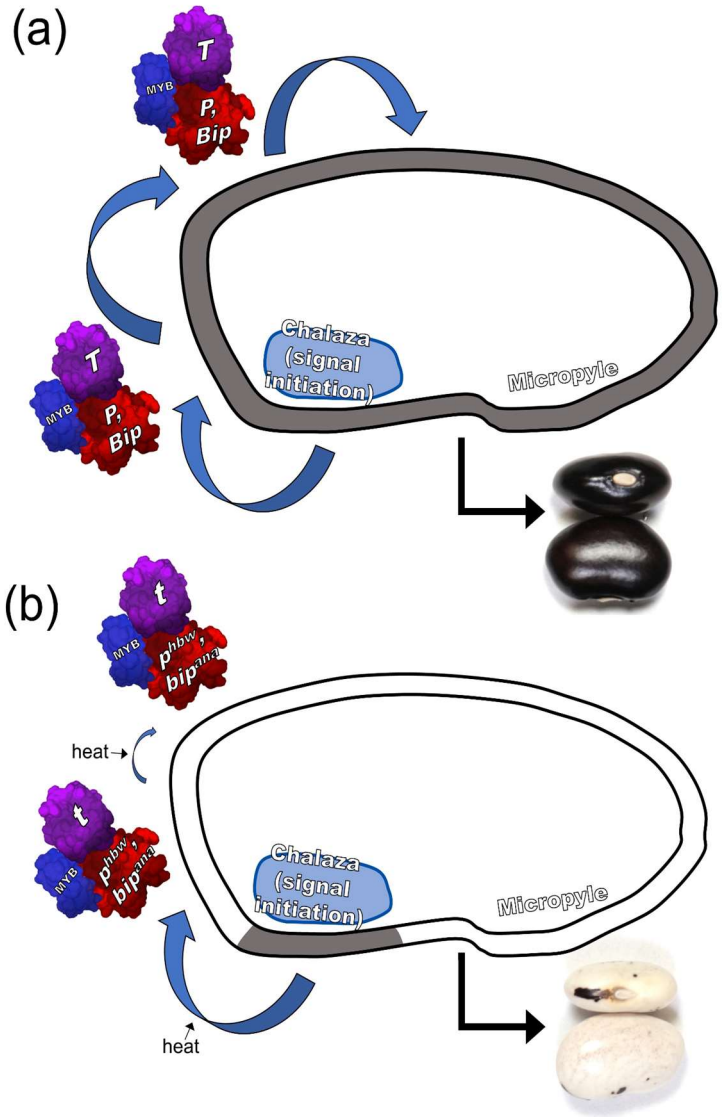

Fig. 8 Model for MBW complex-mediated seed color propagation in *Phaseolus vulgaris*. Signal initiation is known to initiate in the chalaza in Arabidopsis (Baudry et al 2006, Xu et al 2015), and propagate from there by MBW complexes through a self-reinforcing signaling mechanism. In a) wild-type plants of common bean (*T*, *P*, *Bip*), this process leads to phenolic pigment production throughout the seed coat. In b) mutant common beans (*t*, $p^{hbw,}$ and/or bip^{ana}), this signal propagation does not continue effectively beyond the chalaza (on the left of the hilum in the seeds shown), although higher temperatures appear to correspond to greater propagation. (In all the seeds shown, the micropyle is located on the right of the hilum).

thereof) would display the same patterns of environmental instability.

517 ## Parallelism and conclusions

518 In the BXO population, triple mutants produce pigment only at the chalazal end of the seed,
519 where the patterning signal initiates in Arabidopsis. Lines with MBW mutations fail to propagate
520 these signals at various points across the seed coat (Fig. 1). Our results suggest that proteins
521 forming MBW complexes, including *PvTTG1*, *PvMYC1*, and *PvTT8,* are the fundamental
522 propagators of the pigmentation developmental program throughout the seed coat in common
523 bean.

524 These results complement those of this study, showing that common bean seed pattern
525 regulation is determined by interactions between each MBW complex component, with or
526 without interactions with temperature. Other related members of these complexes, including
527 Phvul.003G132100 (*PvTT2*) and Phvul.001G192200 (WDR), will be strong candidates for
528 further detailed exploration (Kavas et al. 2022, Supporting Figs. S).

529 The emerging picture is that genes modifying spatial patterns of pigment deposition—as
530 opposed to pigment composition—appear to encode transcription factors of the MBW
531 complexes. This applies to *T* (*PvTTG1*), *Bip* (*PvMYC1*), *P* (*PvTT8*), *C* (*PvMYB113*), and J
532 (*PvMYB*) and perhaps others such as *Z* (*PvTT2*), and *Sellatus* (*WDR*). Lines carrying mutations at
533 these regulatory genes maintain the metabolic capacity to produce pigments, but the activation of
534 flavonoid pathways does not occur in all cells of the seed coat nor flowers. This stands in
535 contrast to genes controlling pigmentation composition uniformly throughout the seed. These are
536 described as 'color-modifying genes' (Bassett 2007) and may correspond to late biosynthetic
537 genes (Xu et al. 2015, Reinprecht et al. 2013). *Violet* (*V*), for example, is encoded by
538 Phvul.006G018800 (flavonoid 3′5′ hydroxylase; García-Fernández et al. 2021, McClean et al.
539 2022). Other color-modifying genes of this category include *B, G,* and *Rk* (Bassett 2007).

540 The unique alleles and genes described for the first time in this study are key regulators
541 of seed color and pattern formation, and their encoded proteins are predicted to work together in
542 MBW complexes to achieve their effects. Mutations have occurred at each component of these
543 complexes, sometimes in a highly parallel fashion across different ecogeographic races, gene
544 pools, species, and genera. The interactions between mutations in these complexes gives rise to
545 the broad seed diversity found in common bean. Further, this work has also identified

environmental instability across partly-colored varieties of several distinct genetic backgrounds and has shed light on mutations and germplasms that may provide greater color stability. In the future, it will be interesting to compare plant and animal pigmentation and pigmentation pattern and the effect of the environment (Kumar et al. 2022; Elkin et al. 2023; Kratochwil et al. 2023). Deployment of these genetic/genomic resources will be a major step towards maximizing consumer appeal of this important staple crop.

Acknowledgements

This work was financially supported by grants from the Kirkhouse Trust SCIO and the Organic Farming Research Foundation. The plant material is based upon work supported by the U.S. Department of Agriculture Pulse Crop Health Initiative under Agreement No. 58-3060-1-036. Any opinions, findings, conclusion, or recommendations expressed in this publication are those of the author(s) and do not necessarily reflect the view of the U.S. Department of Agriculture. Talissa Floriani Zimmerman assisted with growth chamber studies. JM, MR, MI, and JA helped manage field trials. Steve Temple developed the unreleased "UCD Jacob's Cattle" and "UCD Holstein". Eduardo Blumwald generously provided access to equipment.

Competing interests

None declared.

Author contributions

Initial observations and hypothesis generation: TP, PG

Funding acquisition: TP, PG, CP, LT, GB

Project oversight: TP, PG, CD, GB, LT

Experimental methods: TP, TB, TW, VP, MM, AP, CNJ, MRW, SL, SH, AF

Statistical and computational analysis: TP, TB, TW, SL, AF

Manuscript writing: first draft: TP, PG; subsequent drafts: TP, PG, GB, LT, and CD

All authors approved the final version of the manuscript.

Data availability

Data supporting the findings of this study are available in the Supporting Information of this article. The re-sequence data within 1 Mb of flanking SNPs or previously linked markers will be deposited into the National Center of Biotechnology Information (https://www.ncbi.nlm.nih.gov) with accession no. XXX.

576 ## Supporting information

577

Filename	Description
This file	**Supporting Fig. S1.** Distance tree based on amino acid sequence of AT5G24520.1 (*AtTTG1*) against the NCBI non-redundant *P. vulgaris* and *A. thaliana* proteome database.
	Supporting Fig. S2. Distance tree based on amino acid sequence of AT4G00480.2 (*AtMYC1*) against the non-redundant *P. vulgaris* and *A. thaliana* proteome database at NCBI.
	Supporting Fig. S3. Sequence alignment of Phvul.007G171333.1 (*PvTT8, P*) with homologous transcripts in other legumes.
	Supporting Fig. S4. Distance tree based on amino acid sequence of AT5G35550.2 (*AtTT2*) against *P. vulgaris* and *A. thaliana* proteomes.
	Supporting Fig. S5. Expression of gene models proposed to underlie seed pattern variation in this study.
	Supporting Fig. S6. Relationship between average maximum temperature in July (°C) across field experiments and percent pigmentation of the seed coat. For the sake of comparison, the data obtained in growth chambers in select varieties (labeled GC) are also included.
Supporting Table S1.xlsx	**Supporting Table S1.** Alleles at candidate genes in the 37 sequenced accessions.
Supporting Table S2.xlsx	**Supporting Table S2.** PCR primers, cycling conditions, and restriction digest information.

This file	**Supporting Table S3.** Average proportion of pigmented seed coat area for varieties grown in multilocation trials.
	Supporting Table S4. Average proportion of pigmented seed coat area in growth chamber studies.

578

579 # References

580 **Allen GC, Flores-Vergara MA, Krasynanski S, Kumar S, Thompson WF. 2006.** A modified protocol
581 for rapid DNA isolation from plant tissues using cetyltrimethylammonium bromide. *Nature Protocols*
582 **1**: 2320-2325.

583 **Andrews S 2010**. FastQC: a quality control tool for high throughput sequence data, Available online at:
584 http://www.bioinformatics.babraham.ac.uk/projects/fastqc/: Babraham Bioinformatics, Babraham
585 Institute, Cambridge, United Kingdom.

586 **Bai Q, Li M, Zhou J, Imran A, De Souza TSP, Barrow C, Dunshea F, Suleria HAR. 2023.** Influence
587 of processing methods on phytochemical composition of different varieties of beans (*Phaseolus*
588 *vulgaris*). *Food Reviews International*: 1-39.

589 **Bassett M, Hartel K, McClean P. 2000.** Inheritance of the Anasazi pattern of partly colored seedcoats in
590 common bean. *Journal of the American Society for Horticultural Science* **125**: 340-353.

591 **Bassett MJ. 1996.** New genes, *stp* and stp^{hbw}, for flower and seedcoat pattern in common bean. *Journal of*
592 *the American Society for Horticultural Science* **121**: 388-392.

593 **Bassett MJ. 2003.** Allelism between the *P* and *Stp* genes for seedcoat color and pattern in common bean.
594 *Journal of the American Society for Horticultural Science* **128**: 548-551.

595 **Bassett MJ. 2007.** Genetics of seed coat color and pattern in common bean. *Plant Breeding Reviews* **28**:
596 239-315.

597 **Baudry A, Caboche M, Lepiniec L. 2006.** TT8 controls its own expression in a feedback regulation
598 involving TTG1 and homologous MYB and bHLH factors, allowing a strong and cell-specific
599 accumulation of flavonoids in *Arabidopsis thaliana*. *The Plant Journal* **46**: 768-779.

600 **Baudry A, Heim MA, Dubreucq B, Caboche M, Weisshaar B, Lepiniec L. 2004.** TT2, TT8, and TTG1
601 synergistically specify the expression of BANYULS and proanthocyanidin biosynthesis in
602 *Arabidopsis thaliana*. *The Plant Journal* **39**: 366-380.

603 **Bolger AM, Lohse M, Usadel B. 2014.** Trimmomatic: a flexible trimmer for Illumina sequence data.
604 *Bioinformatics* **30**: 2114-2120.

605 **Brady L, Basset MJ, McClean PE. 1998.** Molecular markers associated with *T* and *Z* , two genes
606 controlling partly colored seed coat patterns in common bean. *Crop Science* **38**: 1073-1075.

607 **Broughton WJ, Hernandez G, Blair M, Beebe S, Gepts P, Vanderleyden J. 2003.** Beans (*Phaseolus*
608 spp.) - model food legumes. *Plant and Soil* **252**: 55-128.

609 **Brouwer BO, Murphy KM, Jones SS. 2016.** Plant breeding for local food systems: A contextual review
610 of end-use selection for small grains and dry beans in Western Washington. *Renewable Agriculture*
611 *and Food Systems* **31**: 172-184.

612 **Darwin C. 1868.** *The variation of plants and animals under domestication*. London: J. Murray.

613 **Elkin J, Martin A, Courtier-Orgogozo V, Santos ME. 2023.** Analysis of the genetic loci of pigment
614 pattern evolution in vertebrates. *Biological Reviews* **98**: 1250-1277.

615 **Erfatpour M, Duizer L, Pauls KP. 2021.** Investigations of the effects of the non-darkening seed coat
616 trait coded by the recessive *jj* alleles on agronomic, sensory, and cooking characteristics in pinto
617 beans. *Crop Science* **61**: 1843-1863.

Erfatpour M, Navabi A, Pauls KP. 2018. Mapping the non-darkening trait from 'Wit-rood boontje' in bean (*Phaseolus vulgaris*). *Theoretical and Applied Genetics* **131**: 1331-1343.

Erfatpour M, Pauls KP. 2020. A R2R3-MYB gene-based marker for the non-darkening seed coat trait in pinto and cranberry beans (*Phaseolus vulgaris* L.) derived from 'Wit-rood boontje'. *Theoretical and Applied Genetics* **133**: 1977-1994.

Ernest EG, Kelly JD, Bassett MJ. 2005. A spontaneous mutation at a seedcoat pattern locus in the dark red kidney bean `Red Hawk,' which changes seed from self-colored to the partially colored virgarcus pattern. *HortScience* **40**: 57-59.

Gálvez Ranilla L, Genovese MI, Lajolo FM. 2007. Polyphenols and antioxidant capacity of seed coat and cotyledon from Brazilian and Peruvian bean cultivars (*Phaseolus vulgaris* L.). *Journal of Agricultural and Food Chemistry* **55**: 90-98.

García-Fernández C, Campa A, Ferreira JJ. 2021. Dissecting the genetic control of seed coat color in a RIL population of common bean (*Phaseolus vulgaris* L.). *Theoretical and Applied Genetics* **134**: 3687-3698.

Goodstein DM, Shu S, Howson R, Neupane R, Hayes RD, Fazo J, Mitros T, Dirks W, Hellsten U, Putnam N, Rokhsar DS. 2012. Phytozome: a comparative platform for green plant genomics. *Nucleic Acids Research* **40**: D1178-D1186.

Herniter IA, Muñoz-Amatriaín M, Lo S, Guo Y-N, Close TJ. 2018. Identification of candidate genes controlling black seed coat and pod tip color in cowpea (*Vigna unguiculata* [L.] Walp). *G3 Genes|Genomes|Genetics* **8**: 3347-3355.

Hufford MB, Berny Mier y Teran JC, Gepts P. 2019. Crop biodiversity: an unfinished magnum opus of nature. *Annual Review of Plant Biology* **70**: 727-751.

Kavas M, Abdulla MF, Mostafa K, Seçgin Z, Yerlikaya BA, Otur Ç, Gökdemir G, Kurt Kızıldoğan A, Al-Khayri JM, Jain SM. 2022. Investigation and expression analysis of R2R3-MYBs and anthocyanin biosynthesis-related genes during seed color development of common bean (*Phaseolus vulgaris*). *Plants* **11**: 3386.

Koenen EJM, Ojeda DI, Bakker FT, Wieringa JJ, Kidner C, Hardy OJ, Pennington RT, Herendeen PS, Bruneau A, Hughes CE. 2020. The origin of the legumes is a complex paleopolyploid phylogenomic tangle closely associated with the Cretaceous–Paleogene (K–Pg) mass extinction event. *Systematic Biology* **70**: 508-526.

Koinange EMK, Singh SP, Gepts P. 1996. Genetic control of the domestication syndrome in common-bean. *Crop Science* **36**: 1037-1045.

Kondratyuk TP, Pezzuto JM. 2004. Natural product polyphenols of relevance to human health. *Pharmaceutical Biology* **42**: 46-63.

Kratochwil CF, Mallarino R. 2023. Mechanisms underlying the formation and evolution of vertebrate color patterns. *Annual Review of Genetics* **57**.

Kumar S, Dar SA, Rani S 2022. Effect of environmental variability on the pigmentation of fishes. In: Sinha A, Kumar S, Kumari K eds. *Outlook of Climate Change and Fish Nutrition*. Singapore: Springer Nature Singapore, 153-170.

Kwak M, Toro O, Debouck D, Gepts P. 2012. Multiple origins of the determinate growth habit in domesticated common bean (*Phaseolus vulgaris* L.). *Annals of Botany* **110**: 1573-1580.

659 **Li H, Durbin R. 2009.** Fast and accurate short read alignment with Burrows–Wheeler transform.
660 *Bioinformatics* **25**: 1754-1760.

661 **McClean PE, Bett KE, Stonehouse R, Lee R, Pflieger S, Moghaddam SM, Geffroy V, Miklas P,**
662 **Mamidi S. 2018.** White seed color in common bean (*Phaseolus vulgaris*) results from convergent
663 evolution in the *P* (pigment) gene. *New Phytologist* **219**: 1112-1123.

664 **McClean PE, Lee RK, Otto C, Gepts P, Bassett MJ. 2002.** Molecular and phenotypic mapping of genes
665 controlling seed coat pattern and color in common bean (*Phaseolus vulgaris* L.). *Journal of Heredity*
666 **93**: 148-152.

667 **O'Rourke JA, Iniguez LP, Fu F, Bucciarelli B, Miller SS, Jackson SA, McClean PE, Li J, Dai X,**
668 **Zhao PX, et al. 2014.** An RNA-Seq based gene expression atlas of the common bean. *BMC*
669 *Genomics* **15**: 866.

670 **Parker T, Palkovic A, Brummer EC, Gepts P. 2021.** Registration of 'UC Southwest Gold' heirloom-
671 like gold and white mottled bean. *Journal of Plant Registrations* **15**: 48-52.

672 **Parker T, Palkovic A, Brummer EC, Gepts P. 2021.** Registration of 'UC Southwest Red' heirloom-like
673 red and white mottled bean. *Journal of Plant Registrations* **15**: 21-27.

674 **Parker T, Palkovic A, Brummer EC, Gepts P. 2021.** Registration of 'UC Sunrise' heirloom-like orange
675 and white mottled bean. *Journal of Plant Registrations* **15**: 43-47.

676 **Parker TA, Gepts P 2021.** Population genomics of *Phaseolus* spp.: A domestication hotspot. In: Rajora
677 OP ed. *Population Genomics: Crop Plants*. Cham, Switzerland: Springer Nature, 1-83.

678 **Parker TA, Palkovic A, Gepts P. 2020.** Determining the genetic control of common bean early-growth
679 rate using unmanned aerial vehicles. *Remote Sensing* **12**: 1748.

680 **R Core Team 2022**. R: A language and environment for statistical computing. Vienna, Austria: R
681 Foundation for Statistical Computing.

682 **Reinprecht Y, Yadegari Z, Perry GE, Siddiqua M, Wright LC, McClean PE, Pauls PK. 2013.** In
683 silico comparison of genomic regions containing genes coding for enzymes and transcription factors
684 for the phenylpropanoid pathway in *Phaseolus vulgaris* L. and *Glycine max* L. Merr. *Frontiers in*
685 *Plant Science* **4**: 317.

686 **Repinski SL, Kwak M, Gepts P. 2012.** The common bean growth habit gene PvTFL1y is a functional
687 homolog of Arabidopsis TFL1. *Theoretical and Applied Genetics* **124**: 1539-1547.

688 **Robinson JT, Thorvaldsdóttir H, Winckler W, Guttman M, Lander ES, Getz G, Mesirov JP. 2011.**
689 Integrative genomics viewer. *Nature Biotechnology* **29**: 24-26.

690 **Rodríguez Madrera R, Campa Negrillo A, Suárez Valles B, Ferreira Fernández JJ. 2020.**
691 Characterization of extractable phenolic profile of common bean seeds (Phaseolus vulgaris L.) in a
692 Spanish diversity panel. *Food Research International* **138**: 109713.

693 **Rose AB. 2019.** Introns as gene regulators: a brick on the accelerator. *Frontiers in Genetics* **9**.

694 **Schmutz J, McClean P, Mamidi S, Wu G, Cannon S, Grimwood J, Jenkins J, Shu S, Song Q,**
695 **Chavarro C, et al. 2014.** A reference genome for common bean and genome-wide analysis of dual
696 domestications. *Nature Genetics* **46**: 707-713.

697 **Shull GH. 1907.** Some latent characters of a white bean. *Science* **25**: 828-832.

Singh B, Singh JP, Shevkani K, Singh N, Kaur A. 2017. Bioactive constituents in pulses and their health benefits. *Journal of Food Science and Technology* **54**: 858-870.

Soler-Garzón A, McClean PE, Miklas PN. 2021. Coding mutations in vacuolar protein-sorting 4 AAA+ ATPase endosomal sorting complexes required for transport protein homologs underlie *bc-2* and new *bc-4* gene conferring resistance to Bean Common Mosaic Virus in common bean. *Frontiers in Plant Science* **12**: 769247.

Soler-Garzón A, McClean PE, Miklas PN. 2021. Genome-wide association mapping of *bc-1* and *bc-u* reveals candidate genes and new adjustments to the host-pathogen interaction for resistance to Bean Common Mosaic Necrosis Virus in common bean. *Frontiers in Plant Science* **12**.

Song Q, Jia G, Hyten DL, Jenkins J, Hwang E-Y, Schroeder SG, Osorno JM, Schmutz J, Jackson SA, McClean PE, Cregan PB. 2015. SNP assay development for linkage map construction, anchoring whole-genome sequence, and other genetic and genomic applications in common bean. *G3: Genes|Genomes|Genetics* **5**: 2285-2290.

Stonehouse R, Tomita A, Bett K 2022. Molecular marker assay from DNA extraction protocol for the USASK Pulse Molecular Biology Laboratory [Lab protocol]. Saskatoon, Canada: University of Saskatchewan.

Swegarden HR, Sheaffer CC, Michaels TE. 2016. Yield stability of heirloom dry bean (*Phaseolus vulgaris* L.) cultivars in Midwest organic production. *HortScience* **51**: 8-14.

Taylor J, Butler D. 2017. R Package ASMap: efficient genetic linkage map construction and diagnosis. *Journal of Statistical Software* **79**: 1-29.

Walters H, Brick MA, Ogg JB. 2011. Evaluation of heirloom beans for production in northern Colorado. *Annual Report of the Bean Improvement Cooperative* **54**: 56-57.

Weller JL, Vander Schoor JK, Perez-Wright EC, Hecht V, González AM, Capel C, Yuste-Lisbona FJ, Lozano R, Santalla M. 2019. Parallel origins of photoperiod adaptation following dual domestications of common bean. *Journal of Experimental Botany* **70**: 1209-1219.

Wu D, Hought J, Baseggio M, Hart JP, Gore MA, Ilut DC. 2019. Genomic characterization of the Native Seeds/SEARCH common bean (*Phaseolus vulgaris* L.) collection and its seed coat patterns. *Genetic Resources and Crop Evolution* **66**: 1469–1482.

Xie X-B, Li S, Zhang R-F, Zhao J, Chen Y-C, Zhao Q, Yao Y-X, You C-X, Zhang X-S, Hao Y-J. 2012. The bHLH transcription factor MdbHLH3 promotes anthocyanin accumulation and fruit colouration in response to low temperature in apples. *Plant, Cell & Environment* **35**: 1884-1897.

Xu W, Dubos C, Lepiniec L. 2015. Transcriptional control of flavonoid biosynthesis by MYB–bHLH–WDR complexes. *Trends in Plant Science* **20**: 176-185.

Yang Q-Q, Gan R-Y, Ge Y-Y, Zhang D, Corke H. 2018. Polyphenols in common beans (*Phaseolus vulgaris* L.): Chemistry, analysis, and factors affecting composition. *Comprehensive Reviews in Food Science and Food Safety* **17**: 1518-1539.

Zhai Y, Yu K, Cai S, Hu L, Amoo O, Xu L, Yang Y, Ma B, Jiao Y, Zhang C, et al. 2020. Targeted mutagenesis of *BnTT8* homologs controls yellow seed coat development for effective oil production in *Brassica napus* L. *Plant Biotechnology Journal* **18**: 1153-1168.

Zhang B, Schrader A. 2017. TRANSPARENT TESTA GLABRA 1-dependent regulation of flavonoid biosynthesis. *Plants (Basel)* **6**.

739

740 What is biodiversity?

741 **Supporting Figures**

742

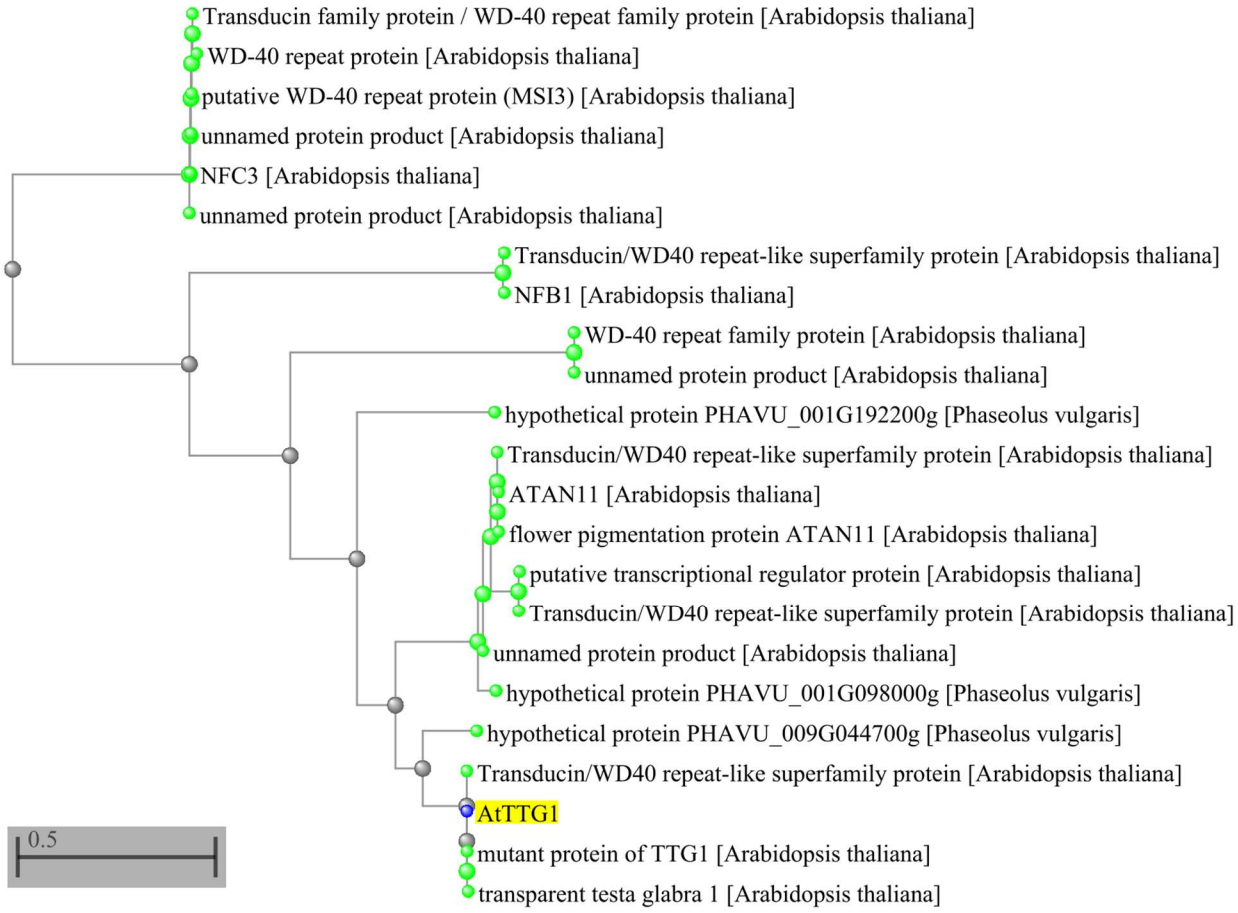

743

744 **Supporting Fig. S1.** Distance tree based on amino acid sequence of AT5G24520.1 (*AtTTG1*)
745 against the NCBI non-redundant *P. vulgaris* and *A. thaliana* proteome database.
746 Phvul.009G044700 (*T* or *PvTTG1*) clusters most closely with *TTG1* of Arabidopsis, indicating
747 that the two are orthologous sister clades among all proteins of the two species.

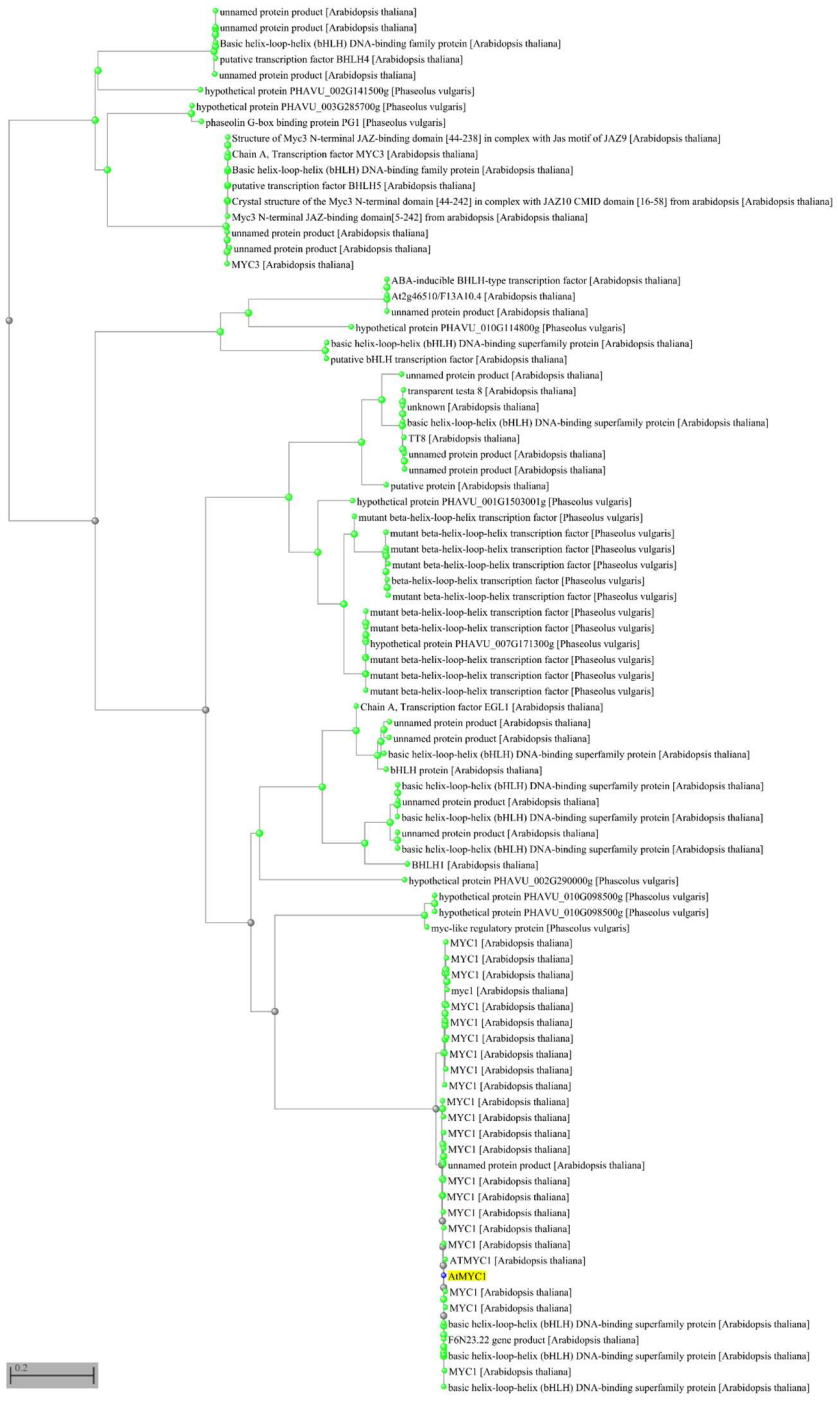

Supporting Fig. S2. Distance tree based on amino acid sequence of AT4G00480.2 (*AtMYC1*) against the non-redundant *P. vulgaris* and *A. thaliana* proteome database at NCBI. Phvul.010G098500 (*Bip* or *PvMYC1*) clusters most closely with *MYC1* of Arabidopsis, indicating that the two are orthologous sister clades among all proteins of the two species.

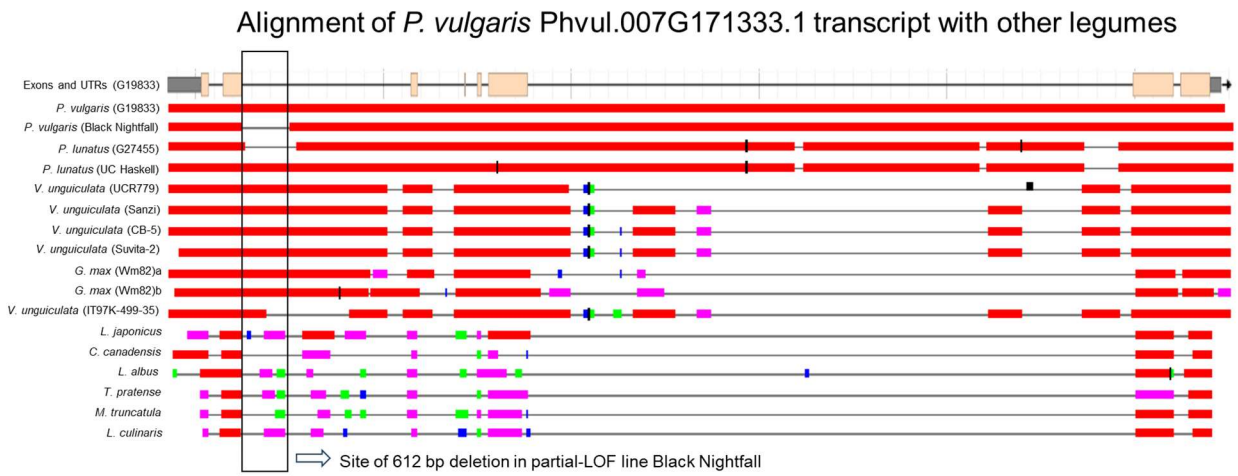

Supporting Fig. S3. Sequence alignment of Phvul.007G171333.1 (*PvTT8, P*) with homologous transcripts in other legumes. An intron sequence deleted in the partially-colored common bean varieties Black Nightfall and Rio Colorado contains motifs that have been conserved even in distantly related legumes of the cool-season IRLC clade and the basal Papilionoid *Lupinus albus* over at least 40 million years of legume evolution (Koenen et al. 2021). The partly-colored reference lima bean (G27455) and partly-colored reference cowpea (IT97K-499-35) also display deletions in the same intron relative to other varieties of those species with no deletions in the area. The deleted regions of partly colored common bean, lima bean, and cowpea are overlapping.

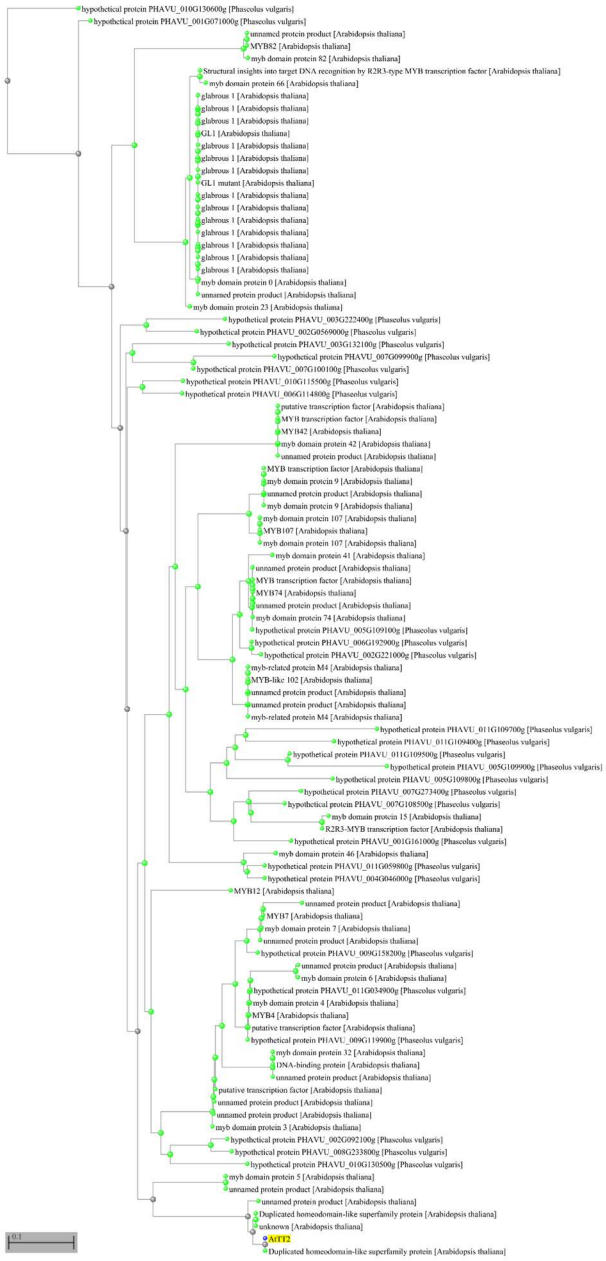

Supporting Fig. S4. Distance tree based on amino acid sequence of AT5G35550.2 (*AtTT2*) against *P. vulgaris* and *A. thaliana* proteomes. *AtTT2* is a critical MBW complex member and regulator of seed coat pigmentation specification in Arabidopsis. Related genes are strong candidates for control of seed coat pigmentation in common bean. Phvul.010G130600 (at top of figure) is an *AtTT2* relative and was recently shown to underpin the *Joker* (*J*) locus in common bean (Erfatpour and Pauls 2020).

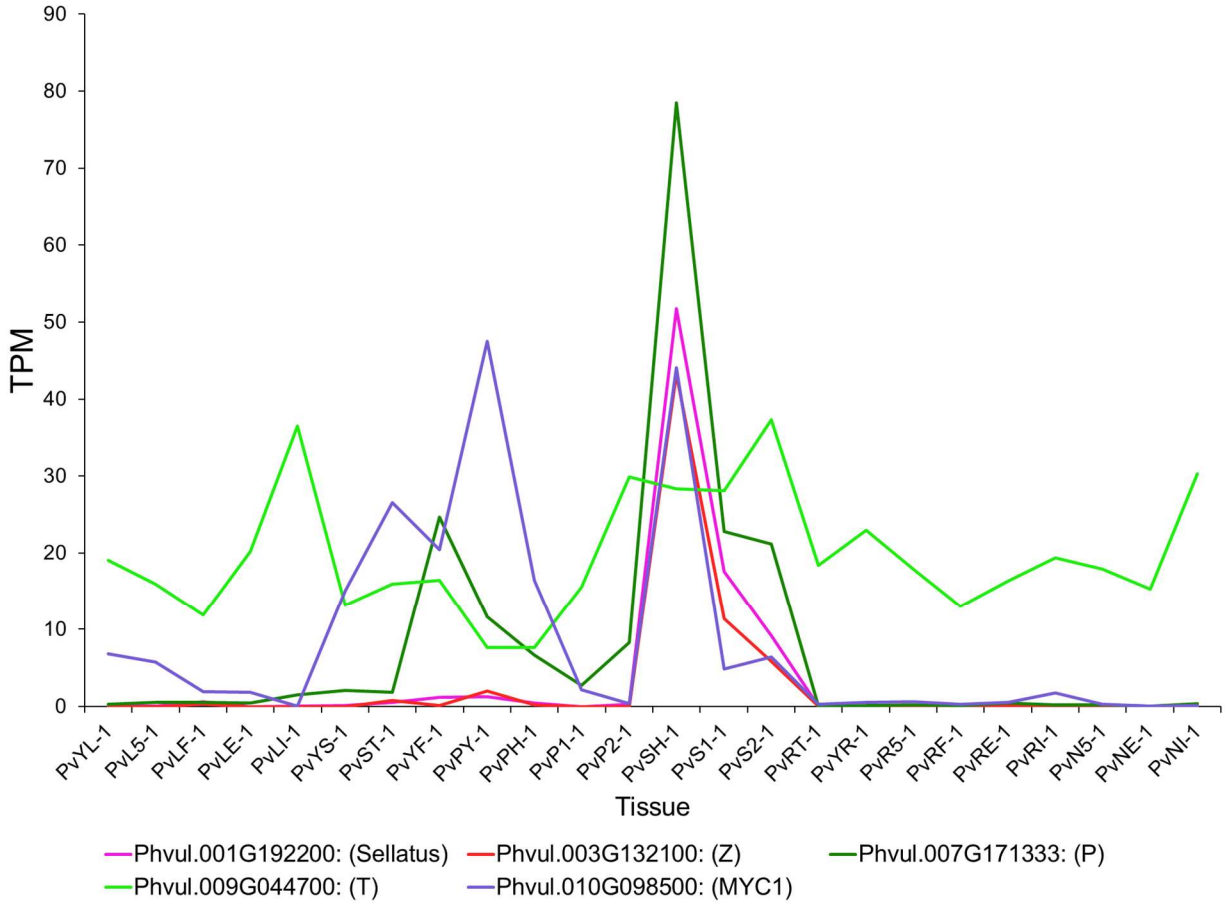

Supporting Fig. S5. Expression of gene models proposed to underlie seed pattern variation in this study. Data are from O'Rourke et al. (2014) and were collected in the genotype 'Black Jamapa' (a Mesoamerican accession). In all cases, very high levels of gene expression occurred in seed development (tissues beginning with 'PvS'). In some cases, the patterns we-re highly correlated, such as between Phvul.001G192200, Phvul.003G132100, and Phvul.007G171333. PvYL - Fully expanded 2nd trifoliate leaf tissue from plants provided with fertilizer. Tissues: PvL5 - Leaf tissue collected 5 days after plants inoculated with effective rhizobium; PvLF - Leaf tissue, fertilized plants; PvLE - Leaf tissue, plants inoculated with effective rhizobium; PvLI - Leaf tissue, plants inoculated with ineffective rhizobium; PvYS - Young stems; PvST - Shoot tip; PvFY - Young flowers; PvPY - Young pods; PvPH - Pods associated with seeds at heart stage (pod only); PvP1 - Pods associated with stage 1 seeds (pod only); PvP2 - Pods associated with stage 2 seeds (pod only); PvSH - Heart stage seeds; PvS1 - Stage 1 seeds; PvS2 - Stage 2 seeds; PvRT - Root tips; PvYR - Young root material, including tips; PvR5 - Whole roots separated from 5 day old pre-fixing nodules; PvRF - Whole roots from fertilized plants; PvRE - Whole roots separated from fix+ nodules; PvRI - Whole roots separated from fix- nodules; PvN5 - Pre-fixing (effective) nodules collected 5 days after inoculation; PvNE - Effectively fixing nodules; PvNI - Ineffectively fixing nodules.

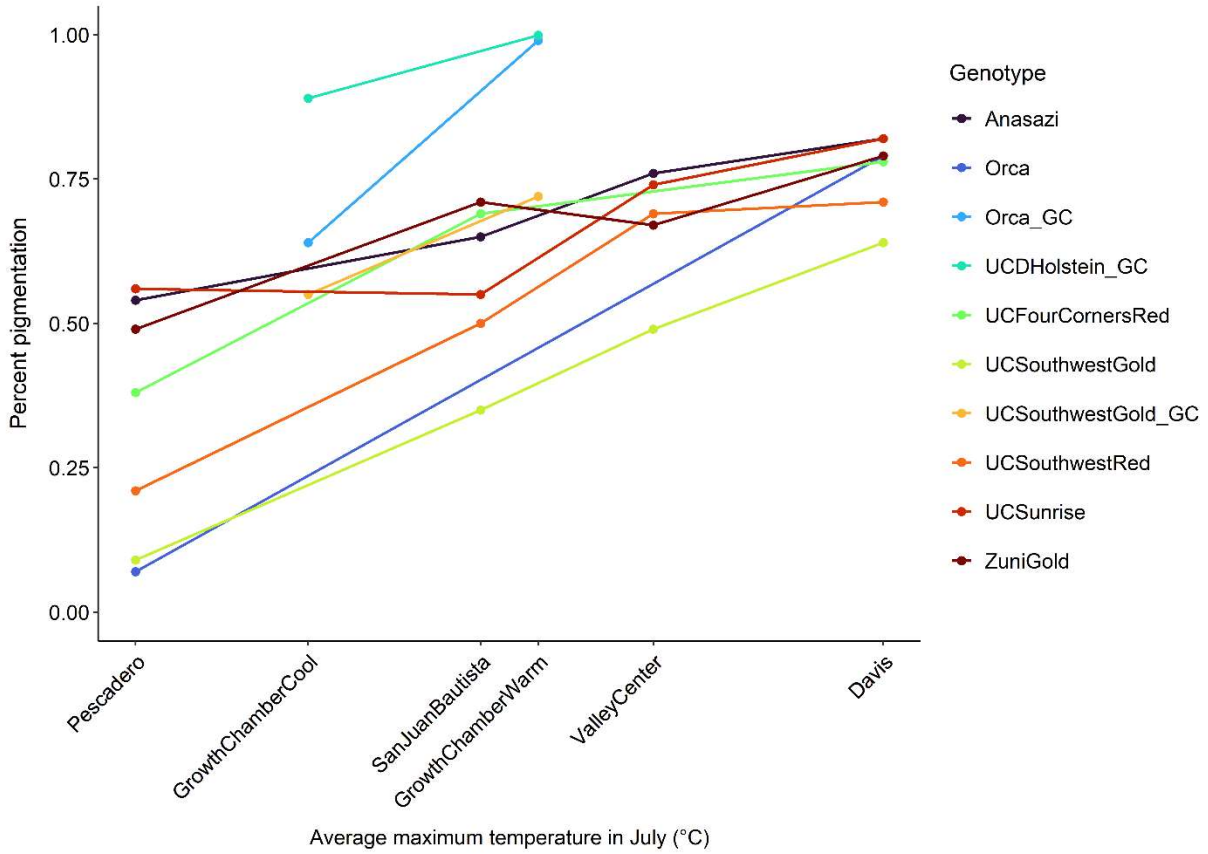

Supporting Fig. S6. Relationship between average maximum temperature in July (°C) across field experiments and percent pigmentation of the seed coat. For the sake of comparison, the data obtained in growth chambers in select varieties (labeled GC) are also included.

794 Supporting Tables

795

796 **Supporting Table S1.** Alleles at candidate gene models in the 37 sequenced accessions.

797

798 In separate file: Supporting Table S1.xlsx

799

800

801

802 **Supporting Table S2.** PCR primers, cycling conditions, and restriction digest information.

803

804 In separate file: Supporting Table S2.xlsx

Supporting Table S3. Average proportion of pigmented seed coat area for varieties grown in multilocation trials.

Location and July temp. (high/low)	Pescadero	San Juan Bautista	Valley Center	Davis
Genotype	21/11 °C	27/12 °C	30/16 °C	34/14 °C
Orca	0.07	-	-	0.79
UC Southwest Gold	0.09	0.35	0.49	0.64
UC Southwest Red	0.21	0.50	0.69	0.71
UC Four Corners Red	0.38	0.69	-	0.78
Zuni Gold	0.49	0.71	0.67	0.79
Anasazi	0.54	0.65	0.76	0.82
UC Sunrise	0.56	0.55	0.74	0.82

Supporting Table S4. Average proportion of pigmented seed coat area in growth chamber studies.

Variety	Cool 24/20 °C	Warm 28/24 °C
UC Southwest Gold	0.55	0.72
Orca	0.64	0.99
UCD Holstein	0.89	0.99

807